Fourier-correlation imaging

Daniel Braun, Younes Monjid, Bernard Rougé, and Yann Kerr

Citation: Journal of Applied Physics **123**, 074502 (2018); doi: 10.1063/1.5017680
View online: https://doi.org/10.1063/1.5017680
View Table of Contents: http://aip.scitation.org/toc/jap/123/7
Published by the American Institute of Physics

JOURNAL OF APPLIED PHYSICS **123**, 074502 (2018)

Fourier-correlation imaging

Daniel Braun,[1,a)] Younes Monjid,[2] Bernard Rougé,[2] and Yann Kerr[2]
[1]*Institute for Theoretical Physics, University Tübingen, 72076 Tübingen, Germany*
[2]*CESBIO, 18 av. Edouard Belin, 31401 Toulouse, France*

(Received 29 November 2017; accepted 29 January 2018; published online 21 February 2018)

We investigated whether correlations between the Fourier components at slightly shifted frequencies of the fluctuations of the electric field measured with a one-dimensional antenna array on board a satellite flying over a plane allow one to measure the two-dimensional brightness temperature as a function of position in the plane. We found that the achievable spatial resolution that resulted from just two antennas is on the order of $h\chi$, with $\chi = c/(\Delta r \omega_0)$, both in the direction of the flight of the satellite and in the direction perpendicular to it, where Δr is the distance between the antennas, ω_0 is the central frequency, h is the height of the satellite over the plane, and c is the speed of light. Two antennas separated by a distance of about 100 m on a satellite flying with a speed of a few km/s at a height of the order of 1000 km and a central frequency of order GHz allow, therefore, the imaging of the brightness temperature on the surface of Earth with a resolution of the order of 1 km. For a single point source, the relative radiometric resolution is on the order of $\sqrt{\chi}$, but, for a uniform temperature field in a half plane left or right of the satellite track, it is only on the order of $1/\chi^{3/2}$, which indicates that two antennas do not suffice for a precise reconstruction of the temperature field. Several ideas are discussed regarding how the radiometric resolution could be enhanced. In particular, having N antennas all separated by at least a distance on the order of the wave-length allows one to increase the signal-to-noise ratio by a factor of order N but requires averaging over N^2 temperature profiles obtained from as many pairs of antennas. *Published by AIP Publishing.* https://doi.org/10.1063/1.5017680

I. INTRODUCTION

Spatial aperture synthesis is a standard technique in radio-astronomy.[1] It allows one to achieve the fine resolution of a large antenna by correlating time-delayed signals received from the different antennas in an antenna array. In satellite-based remote sensing, spatial aperture synthesis is a technique of choice when relatively long wave-lengths are imposed by applications such as the measurement of sea surface salinity or surface soil moisture. When operating in the protected L-band (1400–1427 MHz), a resolution of 10 km would already require a single antenna with a size of 32 m. Spatial aperture synthesis for passive microwave sensing, therefore, was proposed to the European Space Agency (ESA)[2] and implemented for the first time in the “Soil Moisture and Ocean Salinity” (SMOS) mission in 2009, which still operates today.[3,4] The satellite uses a deployable Y-shaped antenna array and provides a spatial resolution between 27 and 60 km.

With the application-driven need for higher spatial resolution down to the order of 1 km, even spatial aperture synthesis leads to forbiddingly large antenna arrays, and, therefore, there is an ongoing quest for finding alternative concepts (see, e.g., Ref. 5 and references therein). Compared with stationary antenna arrays on the Earth used for astronomy, one may wonder whether the motion of the satellite could be used for creating a two-dimensional (2D) artificial antenna array out of a one-dimensional (1D) moving array, oriented perpendicular to the motion of the satellite. It turns out that this is not possible when directly correlating the observed microwave fields in the time domain: the useful phase shift gained due to the motion of the satellite is, to the first order in v_s/c cancelled by the Doppler shift, where v_s is the speed of the satellite and c is the speed of light.[6]

In this paper, we examine another idea: instead of correlating the signals in the time domain, we consider the correlations between their Fourier components at slightly different frequencies. This may seem surprising at first because, at the level of the sources, the standard model assumption is that different frequencies are entirely decorrelated. Nevertheless, a hypothetical monochromatic point source is seen by different antennas at slightly different frequencies due to the slightly different Doppler effect, and, hence, it makes sense to correlate different frequency components from different antennas with each other. The useful frequency differences are tiny, down to below 1 Hz, and correspondingly long acquisition times are needed. However, one may hope that this opens, at least in principle, a new way of achieving a resolution on the order of a kilometer in passive microwave remote sensing in the L-band by using the motion of the satellite for reducing a 2D antenna-array to a 1D array. The principle of the measurement is illustrated in Fig. 1.

We derive the principles of this “Fourier-correlation imaging” (FouCoIm) technique in detail and calculate the achievable spatial and radiometric resolution (RR). An emphasis is put on pushing analytical calculations as far as possible and testing the method at the hand of simple situations, namely, a single point source and a uniform temperature field. An estimation of numerical values is done with a

[a)]Author to whom correspondence should be addressed: daniel.braun@uni-tuebingen.de

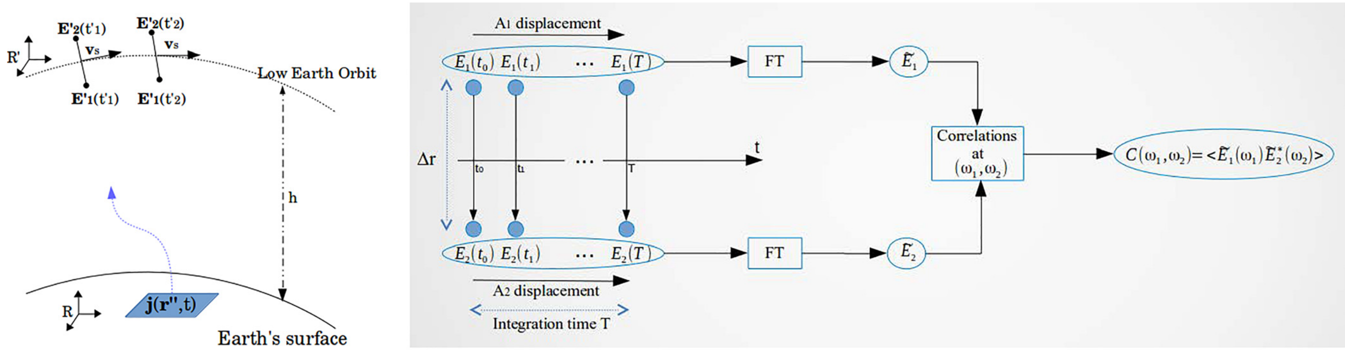

(a) (b)

FIG. 1. Setup of the proposed Fourier-correlation imaging technique. (Left) A satellite comprising at least two antennas flies at height h over the Earth and registers the electric fields $E(\mathbf{r}_i(t), t)$ in the microwave domain, arising from thermally fluctuating current densities on the surface of the Earth, as a function of its proper time t at the time-dependent positions $\mathbf{r}_i(t)$ of the two antennas ($i = 1, 2$). (Right) The two electric fields are Fourier transformed and correlated in a very narrow frequency band (width of order Hz and below). These correlations contain information about the position-dependent brightness temperature on the Earth.

standard set of parameters: $h = 700\,\text{km}$, $v_s = 7\,\text{km/s}$, $\omega_0 = 2\pi \times 1.4\text{GHz}$, $T = 300\text{K}$, $B = 20\text{MHz}$, and $\Delta r = 100\text{m}$. This leads to the important dimensionless parameters $\beta_s = v_s/c = 2.33 \times 10^{-5}$, $\chi = c/(\Delta r \omega_0) = 3.41 \times 10^{-4}$, and $\tilde{h} \equiv h/\Delta r = 7000$.

II. MODEL

We assume that the fluctuating microwave fields measured at the position of the satellite are created by fluctuating microscopic electrical currents at the surface of the Earth that are in local thermal equilibrium at absolute temperature $T(x, y)$, where x, y are coordinates of a point on the surface of the Earth. The entire analysis will be in terms of classical electro-dynamics. In Ref. 6, we derived the expression

$$\mathbf{E}(\mathbf{r}_1 + \mathbf{v}_s t, t) = -\frac{\mu_0}{4\pi} \int d^3r'' \frac{1}{R(t)} \partial_{t'} \mathbf{j}(\mathbf{r}'', t')|_{t'=t-R(t)/c}, \quad (1)$$

for the time-dependent electric field that arises from the current fluctuations at the position of the satellite, with $R(t) = |\mathbf{r}_1 + \mathbf{v}_s t - \mathbf{r}''|$, where $\mathbf{r}_1$ is the position of the antenna at time $t = 0$, $\mathbf{v}_s$ is the speed of the satellite in the Earth-fixed reference frame, μ_0 is the magnetic permeability of a vacuum, and $\mathbf{j}(\mathbf{r}'', t)$ is the current density as a function of space and time. All expressions are in the Earth-fixed reference frame, which is more convenient for the present study than the satellite-fixed reference frame. It is shown in Ref. 6 that Eq. (1) is the correct far field, when relativistic corrections of the prefactor of order β_s (due to the mixing of electric and magnetic fields in a moving reference frame), and terms of order β_s^2 in the phase are neglected. Equation (1) contains, in the phase, the linear Doppler shift and relativistic effects (including time dilation) up to the order β_s. The far-field approximation is justified for $R(t) \gg \lambda$, where λ (on the order of cm in the microwave regime) is the wave-length of the radiation (see Chap. 9 in Ref. 7).

We substitute the Fourier decomposition of the current density,

$$\mathbf{j}(\mathbf{r}'', t) = \frac{1}{\sqrt{2\pi}} \int_{-\infty}^{\infty} d\omega' e^{i\omega' t} \tilde{\mathbf{j}}(\mathbf{r}'', \omega'), \quad (2)$$

into (1). The question of whether one should differentiate $R(t)$ with respect to t was answered to the negative in Ref. 6, but it is irrelevant if we neglect changes of the order β_s to the prefactor. We then find the time-dependent field seen by the flying antenna,

$$\mathbf{E}_{\mathbf{r}_1}(t) \equiv \mathbf{E}(\mathbf{r}_1 + \mathbf{v}_s t, t) = \frac{K_1}{\sqrt{2\pi}} \int d^3r'' \times \int d\omega' \frac{i\omega'}{|\mathbf{r}_1 + \mathbf{v}_s t - \mathbf{r}''|} \tilde{\mathbf{j}}(\mathbf{r}'', \omega') e^{i\omega'(t - |\mathbf{r}_1 + \mathbf{v}_s t - \mathbf{r}''|/c)}, \quad (3)$$

with $K_1 = -\mu_0/(4\pi)$. The Fourier transform of that signal is

$$\tilde{\mathbf{E}}_{\mathbf{r}_1}(\omega_1) = \frac{1}{\sqrt{2\pi}} \int_{-\infty}^{\infty} dt_1 e^{-i\omega_1 t_1} \mathbf{E}_{\mathbf{r}_1}(t_1), \quad (4)$$

$$= \frac{K_1}{2\pi} \int_{-\infty}^{\infty} dt_1 \int_{-\infty}^{\infty} d\omega' \int d^3r'' \frac{i\omega' \tilde{\mathbf{j}}(\mathbf{r}'', \omega')}{|\mathbf{r}_1 + \mathbf{v}_s t_1 - \mathbf{r}''|} \times e^{i(\omega' - \omega_1)t_1} e^{-i\omega'|\mathbf{r}_1 + \mathbf{v}_s t_1 - \mathbf{r}''|/c}. \quad (5)$$

We assume that the current sources can be described by a Gaussian process, in which sources at different positions or different frequencies, or with different polarizations are uncorrelated,

$$\langle \tilde{j}_i(\mathbf{r}_1'', \omega_1) \tilde{j}_j^*(\mathbf{r}_2'', \omega_2) \rangle = \delta_{ij} \frac{l_c^3}{\tau_c} \delta(\mathbf{r}_1'' - \mathbf{r}_2'') \delta(\omega_1 - \omega_2) \langle |\tilde{j}_i(\mathbf{r}_2'', \omega_2)|^2 \rangle, \quad (6)$$

where we introduced, for dimensional grounds, a correlation length l_c and a correlation time τ_c, and the polarizations are indexed by i, j, which take values x, y, z. In principle, the average $\langle \ldots \rangle$ is over an ensemble of realizations of the stochastic process, but we may assume ergodicity of the fluctuations, such that they can also be obtained from a sufficiently long temporal average. In practice, this means that one should average over positions considered as equivalent in terms of the ensemble, i.e., the time that the satellite takes to fly over a desired pixel size. For a satellite flying at a speed on the order of km/s and a pixel size on the order of km, this means a maximal averaging time on the order of a second. This does not preclude calculating Fourier transforms with finer spectral resolution from data acquired over much longer times.

We make the assumption that only the current intensities at the surface of the Earth contribute. In reality, the emission seen by the satellite arises from a thin surface layer on the Earth that has a finite thickness d on the order of a few centimeters,[4,8] depending on the soil and its humidity, and the satellite also sees the cosmic microwave background. We approximate the surface layer as a single plane located at $z''=0$, i.e., $\langle|\tilde{j}_i(\mathbf{r}''_2,\omega_2)|^2\rangle = d\langle|\tilde{j}_i(x'',y'',\omega_2)|^2\rangle\delta(z'')$, and neglect the cosmic microwave background because its temperature is two orders of magnitude lower than that of the Earth as well as other astronomical objects.

The current intensities are related to an effective temperature $T(x, y)$ by

$$\langle|\tilde{j}_i(x,y,\omega)|^2\rangle = K_2 T(x,y)\,, \tag{7}$$

where K_2 is a constant [see Eq. (A11)]. Equation (7) is valid for $\hbar\omega \ll k_B T$ and, hence, well adapted to microwave emission at room temperature.

Equation (6) together with (7) is a standard model of classical white noise currents, and appears in many places in the literature, see e.g., Eq. (4.16) in Ref. 9. The equation is an instance of the fluctuation-dissipation theorem that can be found in standard text-books on statistical physics (see e.g., Part 1, Chap. XII, and Part 2, Chap. VIII in Ref. 10). In the context of thermal radiation, it goes back at least to the original Russian version of Ref. 11 (from 1953); see also Ref. 12. The model has also been used to study coherence effects in the thermal radiation of near-fields [see Eq. (3) in Ref. 13]. For completeness and in preparing the proof that the Fourier components $\tilde{E}_{\mathbf{r}_1}(\omega_1)$ represent a complex circular Gaussian process over position and frequency, we present the derivation of (7) in Appendix A–D, based on Planck's law for the energy density of an electromagnetic (e. m.) field in thermal equilibrium.

Compared with a black body, the emissivity of a real body is modified by a mode-dependent emissivity factor $B_i(x,y;\omega,\hat{k})$, where $\hat{k}$ is the direction of emission (from the patch on the ground to the satellite) and a factor $\cos\theta(x,y,h)$ of geometrical origin that takes into account the variation of the radiation with respect to the normal surface (i.e., the projection of the area of a patch of the surface onto the plane perpendicular to the propagation direction). The temperature $T(x, y)$ is then really an effective temperature, $T_{\rm eff}(x,y) = T_B(x,y)\cos\theta(x,y,h)$, where the brightness temperature $T_B(x,y)$ is defined as the absolute temperature that a black-body would need to have to produce the same intensity of radiation at the frequency and in the direction considered (see Appendix A 1). For simplifying notations, in the rest of the paper, we write $T(x, y)$ for short instead of $T_{\rm eff}(x,y)$, but keep in mind its physical meaning, which, after all, is crucial for data analysis and fitting vegetation and surface models to observational data.[8] We thus arrive at the current correlator

$$\langle\tilde{j}_i(\mathbf{r}''_1,\omega_1)\tilde{j}^*_j(\mathbf{r}''_2,\omega_2)\rangle = \delta_{ij}K_3\,\delta(\mathbf{r}''_1-\mathbf{r}''_2)\delta(\omega_1 - \omega_2)T(x'',y'')\delta(z'')\,, \tag{8}$$

which can be considered the statistical model that underlies the imaging concept, and $K_3 = l_c^3 K_2 d/\tau_c$.

III. CORRELATION OF FOURIER COMPONENTS

For each antenna, the electric field component $E_{i,\mathbf{r}_1}(t)$ is transduced into a voltage $U_{i,\mathbf{r}_1}(t)$. We denote the frequency response of the antennas and the eventual subsequent filters by the complex function $A(\omega)$, the Fourier transform of the time-dependent response function of the antenna and filter. In the frequency domain, we simply have $\tilde{U}_{i,\mathbf{r}_1}(\omega_1) = A(\omega_1)\tilde{E}_{i,\mathbf{r}_1}(\omega_1)$. With (8) we obtain the correlation function between the voltages at two different frequency components, ω_1, ω_2, measured at the positions of the antennas with the original positions $\mathbf{r}_1$ and $\mathbf{r}_2$,

$$\begin{aligned} C^F_{ij}(\mathbf{r}_1,\mathbf{r}_2,\omega_1,\omega_2) &\equiv \langle\tilde{U}_{i,\mathbf{r}_1}(\omega_1)\tilde{U}^*_{j,\mathbf{r}_2}(\omega_2)\rangle \\ &= C_{ij}(\mathbf{r}_1,\mathbf{r}_2,\omega_1,\omega_2)A(\omega_1)A^*(\omega_2), \end{aligned} \tag{9}$$

$$C_{ij}(\mathbf{r}_1,\mathbf{r}_2,\omega_1,\omega_2) = \langle\tilde{E}_{i,\mathbf{r}_1}(\omega_1)\tilde{E}^*_{j,\mathbf{r}_2}(\omega_2)\rangle, \tag{10}$$

$$\begin{aligned} &= K_5\delta_{ij}\int_{-\infty}^{\infty}dt_1\int_{-\infty}^{\infty}dt_2\int_{-\infty}^{\infty}d\omega'\int dx''dy'' \\ &\times\frac{\omega'^2 T(x'',y'')}{|\mathbf{r}_1+\mathbf{v}_s t_1-\mathbf{r}''||\mathbf{r}_2+\mathbf{v}_s t_2-\mathbf{r}''|}\times e^{i\omega'(t_1-t_2)} \\ &\times e^{-i(\omega_1 t_1-\omega_2 t_2)}e^{-i\frac{\omega'}{c}(|\mathbf{r}_1+\mathbf{v}_s t_1-\mathbf{r}''|-|\mathbf{r}_2+\mathbf{v}_s t_2-\mathbf{r}''|)}, \end{aligned} \tag{11}$$

where now $\mathbf{r}'' = (x'',y'',0)$, and $K_5 = K_3K_1^2/(4\pi^2)$. The correlation function $C^F_{ij}(\mathbf{r}_1,\mathbf{r}_2,\omega_1,\omega_2)$ is the filtered version of the original unfiltered correlations $C_{ij}(\mathbf{r}_1,\mathbf{r}_2,\omega_1,\omega_2)$. We see from (9) that the latter can be obtained from the former simply by dividing through the product of the known filter functions, as long as the latter is non-zero. Outside the frequency response of the antennas and filters, the measured correlations $C^F_{ij}(\mathbf{r}_1,\mathbf{r}_2,\omega_1,\omega_2)$ vanish due to the vanishing of $A(\omega)$ and no longer carry any information. This will ultimately limit the frequency range over which information on the brightness temperature can be extracted or, equivalently, leads to a finite geometrical resolution, even if a $C_{ij}(\mathbf{r}_1,\mathbf{r}_2,\omega_1,\omega_2)$ known for all frequencies would lead to perfect resolution. However, this appears only when inverting the measured signals and will be discussed in Sec. IV A. For the moment, we assume that we have access to the unfiltered $C_{ij}(\mathbf{r}_1,\mathbf{r}_2,\omega_1,\omega_2)$ through (9) for all frequencies that we need and base the general development of the theory on $C_{ij}(\mathbf{r}_1,\mathbf{r}_2,\omega_1,\omega_2)$.

We change integration variables from t_1, t_2 to "center-of-mass" and relative times, $t=(t_1+t_2)/2$ and $\tau=(t_2 - t_1)$, and introduce as well, a new integration variable for the spatial integration, $\mathbf{r}' \equiv \mathbf{r}'' - \mathbf{v}_s t$. This implies $\mathbf{r}_1+\mathbf{v}_s t_1 - \mathbf{r}'' = \mathbf{r}_1 - \mathbf{v}_s\tau/2 - \mathbf{r}'$ and $\mathbf{r}_2+\mathbf{v}_s t_2-\mathbf{r}'' = \mathbf{r}_2+\mathbf{v}_s\tau/2-\mathbf{r}'$. The Jacobian of both transformations is equal to 1. Furthermore, from now on, we take the satellite to move in the x-direction, $\mathbf{v}_s = v_s\hat{e}_x$, where $\hat{e}_x$ is the unit vector in the x-direction. This leads to $T(x'',y'') = T(x'+v_s t, y')$.

The total phase Φ appearing as arguments of the exponential functions under the integrals in (11) is

$$i\Phi = i\left[\tau\left(-\omega' + \frac{\omega_2+\omega_1}{2}\right) + t(\omega_2-\omega_1) - \frac{\omega'}{c}\left(|\mathbf{r}_1 - \mathbf{v}_s\tau/2 - \mathbf{r}'| - |\mathbf{r}_2 + \mathbf{v}_s\tau/2 - \mathbf{r}'|\right)\right]. \quad (12)$$

We see that t only appears as a prefactor of $(\omega_2-\omega_1)$ in the phase (12) and as the argument $\mathbf{v}_s t$ in $T(x'+v_x t, y')$. Therefore, the integral over t boils down to a 1D Fourier transform of the intensity of the current fluctuations in the direction of the speed of the satellite, with a conjugate variable proportional to the difference $\omega_2-\omega_1$ of the frequencies of the Fourier components that we correlate. This can be made more explicit by introducing a position variable, $x = v_{st}$, along the path of the satellite. For the conjugate variable, we define $\kappa_x = (\omega_2-\omega_1)/v_s$. We write κ_x and not k_x to distinguish this "wavevector" from the usual one obtained from a single frequency and by dividing by c. We also introduce the "center of mass frequency" $\omega_c \equiv (\omega_1+\omega_2)/2$. It is called "center frequency" for short in the rest of the paper but should not be confused with the central frequency ω_0, which is the fixed frequency in the middle of the band in which the satellite operates (e.g., $2\pi\times$ 1.4 GHz for the SMOS satellite of ESA). With all this, we see that

$$\int T(x'+v_s t, y')e^{i(\omega_2-\omega_1)t}dt = \frac{1}{v_s}\int T_{\mathbf{r}'}(x)e^{i\kappa_x x}\,dx = \frac{\sqrt{2\pi}}{v_s}\tilde{T}_{\mathbf{r}'}(\kappa_x), \quad (13)$$

$$\equiv \frac{\sqrt{2\pi}}{v_s}\tilde{T}_{x',y'}(\kappa_x)\,. \quad (14)$$

We defined $T(x'+v_s t, y') \equiv T_{\mathbf{r}'}(x)$, where $v_s t = x$ is understood, and the spatial Fourier transform $\tilde{T}_{\mathbf{r}'}(\kappa_x)$ of the temperature field $T(x, y)$ is in the x-direction. This notation makes clear that, with these coordinates, the temperature depends both on $\mathbf{r}'$ and t, even though the motion of the satellite combines the two arguments into a single one, $\mathbf{r}' + \mathbf{v}_s t$. We can think of $\tilde{T}_{\mathbf{r}'}(\kappa_x)$ as the Fourier image of $T(\mathbf{r}' + x\hat{e}_x)$ with respect to the x coordinate, calculated with a starting point $\mathbf{r}'$; i.e., for all $\mathbf{r}'$, we have a 1D spatial Fourier transform of the intensity of the current fluctuations, where the Fourier integral is defined with origin in $\mathbf{r}'$. The Fourier images obtained by translation of $\mathbf{r}'$ in the x-direction are not independent. Rather, we have

$$\tilde{T}_{x',y'}(\kappa_x) = \frac{1}{\sqrt{2\pi}}\int dx T_{x',y'}(x)e^{i\kappa_x x} = \frac{1}{\sqrt{2\pi}}\int dx T_{0,y'}(x+x')e^{i\kappa_x x}, \quad (15)$$

$$= \frac{1}{\sqrt{2\pi}}\int dx'' T_{0,y'}(x'')e^{i\kappa_x x''}e^{-i\kappa_x x'} = e^{-i\kappa_x x'}\tilde{T}_{0,y'}(\kappa_x)\,. \quad (16)$$

We are thus led to

$$C_{ij}(\mathbf{r}_1,\mathbf{r}_2,\omega_1,\omega_2) = K_5\delta_{ij}\frac{\sqrt{2\pi}}{v_s}\int_{-\infty}^{\infty}d\tau\int_{-\infty}^{\infty}d\omega'\omega'^2\int dx'\,dy' \times \frac{\tilde{T}_{0,y'}(\kappa_x)e^{-i\kappa_x x'}}{|\mathbf{r}_1 - \mathbf{v}_s\tau/2 - \mathbf{r}'||\mathbf{r}_2 + \mathbf{v}_s\tau/2 - \mathbf{r}'|} \times \exp\left\{i\left[\tau\left(-\omega' + \frac{\omega_2+\omega_1}{2}\right) - \frac{\omega'}{c}\left(|\mathbf{r}_1 - \mathbf{v}_s\tau/2 - \mathbf{r}'| - |\mathbf{r}_2 + \mathbf{v}_s\tau/2 - \mathbf{r}'|\right)\right]\right\}. \quad (17)$$

We neglect the slow dependence of ω'^2 compared with the rapid oscillations of the phase factors in (17) and pull it out of the integral as a prefactor ω_0^2. We can then perform the integral over ω', and we find

$$\int_{-\infty}^{\infty}\exp\left[\ldots\right]d\omega' = 2\pi\delta\left[\tau + \frac{1}{c}\left(|\mathbf{r}_1 - \mathbf{v}_s\tau/2 - \mathbf{r}'| - |\mathbf{r}_2 + \mathbf{v}_s\tau/2 - \mathbf{r}'|\right)\right]e^{i\tau\frac{\omega_1+\omega_2}{2}}\,. \quad (18)$$

We introduce center-of-mass and relative coordinates for $\mathbf{r}_1$ and for $\mathbf{r}_2$, $\mathbf{R} = (\mathbf{r}_1+\mathbf{r}_2)/2$ and $\Delta\mathbf{r} = \mathbf{r}_2 - \mathbf{r}_1$. We further restrict $v_s\tau$ to values much smaller than $|\mathbf{R} - \mathbf{r}'\pm\Delta r|$. This implies a limitation of the integration range for τ when calculating the Fourier components; however, it is mild. Because $|\mathbf{R} - \mathbf{r}'\pm\Delta r| \geq h$, it is enough to have $\tau \leq h/v_s$, which is typically on the order of 100s and, therefore, gives time to resolve Fourier components down to a hundredth of a Hertz. We can then approximate to the first order in v_s,

$$|\mathbf{r}_1 - \mathbf{v}_s\tau/2 - \mathbf{r}'| - |\mathbf{r}_2 + \mathbf{v}_s\tau/2 - \mathbf{r}'| \simeq -\hat{e}_{\mathbf{R}-\mathbf{r}'}\cdot(\Delta\mathbf{r} + \mathbf{v}_s\tau)\,. \quad (19)$$

Neglecting terms on the order of $|\Delta\mathbf{r} + \mathbf{v}_s\tau|/|\mathbf{R} - \mathbf{r}'|$ and on the order of $\beta = v_s/c$ in the prefactor of the exponential as well as a second order term on the order of $\beta\omega_c\Delta r/c$ in the phase, the integral over the Dirac δ-function gives

$$C_{ij}(\mathbf{r}_1,\mathbf{r}_2,\omega_1,\omega_2) = K_6\delta_{ij}\int_{-\infty}^{\infty}dx'\int_{-\infty}^{\infty}dy'\frac{\tilde{T}_{0,y'}(\kappa_x)e^{-i\kappa_x x'}}{|\mathbf{R} - \mathbf{r}'|^2} \times \exp\left[i\frac{\Delta\mathbf{r}\cdot\hat{e}_{\mathbf{R}-\mathbf{r}'}}{c}\omega_c\right], \quad (20)$$

and $K_6 = (2\pi)^{3/2}\omega_0^2 K_5/v_s$. The unit vector $\hat{e}_{\mathbf{R}-\mathbf{r}'}$ is obtained by taking the original center-of-mass position of the antennas at $\mathbf{R} = (x_0, 0, h)$, and $\mathbf{r}' = (x', y', 0)$. Equation (20) is one of the central results of this paper. It shows that the two-frequency correlation function of the fields at different antenna positions is related linearly via a 2D integral transformation to the brightness temperature field in the source plane or, more precisely, to the Fourier transform of that field in the x-direction. With $T(x, y)$ defined on a 2D grid, the reconstruction of $T(x, y)$ from the measured correlation function thus becomes a matrix inversion problem that, in general, has to be performed numerically. A crucial question is the conditioning of the inversion problem. It will be studied in more detail in a subsequent paper dedicated to a numerical approach.[14]

Here we give a simplified analytical treatment that allows us to obtain estimates of the spatial and radiometric resolutions, and thus provide evidence that the inversion problem is sufficiently well conditioned for the reconstruction of $T(x, y)$ from the measured $C_{i,j}(\mathbf{r}_1, \mathbf{r}_2, \omega_1, \omega_2)$. For this, we study the situation in which the vector $\Delta\mathbf{r}$ from antenna 1 to antenna 2 is orientated in the y' direction, $\mathbf{r}_2 = \mathbf{r}_1 + \Delta r\hat{e}_y$, in which case, $\Delta\mathbf{r}\cdot\hat{e}_{\mathbf{R}-\mathbf{r}'} = -\Delta r y'/\sqrt{(x'-x_0)^2 + y'^2 + h^2}$, and $\Delta r = |\Delta\mathbf{r}|$ denotes the spatial separation of the two antennas.

We switch to a dimensionless representation by taking as the length scale the distance Δr between the two antennas. We express all other lengths in this unit and introduce the dimensionless coordinates ξ, η by $x' = \xi\Delta r$, $y' = \eta\Delta r$, and $\tilde{h} \equiv h/\Delta r$. The dimensionless height $\tilde{h}$ is for the standard parameters $\tilde{h} = 7\times 10^3$. Equation (20) then reads

$$\begin{aligned} &C_{ij}(\mathbf{r}_1, \mathbf{r}_1 + \Delta r\hat{e}_y, \omega_1, \omega_2) \\ &= K_6\delta_{ij}e^{-i\kappa_x x_0}\int_{-\infty}^{\infty}\frac{d\eta}{\sqrt{\eta^2+\tilde{h}^2}} \\ &\times K\left(\kappa_x\Delta r\sqrt{\eta^2+\tilde{h}^2}, \frac{\Delta r\omega_c}{c}\frac{\eta}{\sqrt{\eta^2+\tilde{h}^2}}\right)\tilde{T}(\kappa_x, \eta), \end{aligned} \tag{21}$$

where $\tilde{T}(\kappa_x, \eta) \equiv \tilde{T}_{0,\eta\Delta r}(\kappa_x)$. The 1D integral kernel is

$$K(\alpha, \beta) = \int_{-\infty}^{\infty} d\xi \frac{e^{-i\left(\alpha\xi + \frac{\beta}{\sqrt{\xi^2+1}}\right)}}{\xi^2+1}, \tag{22}$$

which is itself defined through an integral over ξ. For fixed h, Δr, ω_c, and κ_x, the integral kernel $K(\alpha,\beta)$ is a function of η that relates the 1D Fourier transform $\tilde{T}(\kappa_x, \eta)$ to the observed correlation function by integration over η. Suppose that the integration over η can be inverted by finding the inverse integral kernel. Integrating over the product of the inverse kernel and the measured correlation function expressed as a function of the center frequency ω_c, we then obtain $\tilde{T}_{0,\Delta r\eta}(\kappa_x)$ for all η and the chosen κ_x. If this can be done for all relevant κ_x, we obtain for each point on the y axis the Fourier transform in the x-direction of the intensity of the brightness temperature. When taking the inverse Fourier transform in the x-direction, we obtain the full x- and y-dependent brightness temperatures.

The arguments α and β of K are given by Eq. (21) as

$$\alpha = \kappa_x\Delta r\sqrt{\eta^2+\tilde{h}^2}, \tag{23}$$

$$\beta = \frac{\Delta r\omega_c}{c}\frac{\eta}{\sqrt{\eta^2+\tilde{h}^2}}. \tag{24}$$

Their physical meanings are as follows: α can be seen as essentially the separation Δr between the two antennas in units of the effective wave-length $1/\kappa_x$ used for Fourier transformation of the temperature profile in the x-direction, multiplied with a dimensionless measure of the distance of the sources from the satellite. We recall that $\kappa_x = (\omega_2 - \omega_1)/v_s$, i.e., the effective wave-length is chosen by fixing the small frequency difference $\omega_2 - \omega_1$. This difference is translated into a wave-vector not by division with the speed of light but by the much smaller speed of the satellite. The latter fact, combined with the large dimensionless distance ($\sqrt{y^2+h^2}$ in units of Δr, which is the meaning of $\sqrt{\eta^2+\tilde{h}^2}$), indicates that α need not be very small even for $\omega_2 - \omega_1$ on the order of 1 Hz.

The parameter β depends, at least for $y > h$, only weakly on the position due to the factor $\eta/\sqrt{\eta^2+\tilde{h}^2} = y/\sqrt{y^2+h^2}$. For $y \ll h$, it is to the first order in η (with $\eta \ll 1$ in that regime) equal to y/h. The other factors in β, $\Delta r\omega_c/c$ just give $k_c\Delta r$ where $k_c = \omega_c/c$ is the wave-vector that corresponds to the central frequency. In other words, up to a factor 2π, the ratio $\Delta r\omega_c/c$ is just the distance between the two antennas in units of the central wave-length.

By their definition, we only need $\alpha, \beta \in \mathbb{R}$. For α, we can consider that, in the end, the maximum κ_x should be on the order of the inverse resolution $\Delta x_{\min}$ required in the x-direction. When taking $\Delta x_{\min}$ on the order of 1 km and when using the standard parameters, we get $|\alpha|_{\max} \geq |\kappa_x h| \simeq 700$. With η varying from $-\infty\ldots\infty$ (in reality, the extension of the Earth limits the integration range to a maximum value on the order of $10^7 - 10^8$), β reaches its maximal value $\Delta r\omega_c/c$ for $\eta\to\infty$. For standard parameters, $\omega_c = 2\pi\times 1.4$ GHz, $|\beta| \lesssim 30$. Both α and β can be positive or negative, such that there is also a regime where $|\beta| \gg |\alpha|$, and, by studying the properties of the kernel $K(\alpha,\beta)$ (see Appendix B), we find that this is the most important regime. There, the kernel essentially becomes independent of α and can be approximated as

$$K(\alpha,\beta) \simeq \sqrt{\frac{2\pi}{\beta}}e^{i\pi/4}e^{-i\beta}, \tag{25}$$

valid for $\beta/\alpha \gg 1$ [see Eq. (B5)].

IV. ESTIMATION OF GEOMETRICAL RESOLUTION

A. Approximate analytical inversion of the integral kernel

At first sight, the requirement $\beta \gg \alpha$ appears unnatural, given that α can already be on the order of 10^2 to 10^3. Indeed, this leads to a first rather stringent condition that must be met for the correlation function C to be non-zero. In terms of the original parameters, $\beta/\alpha = \omega_c\eta/[c\kappa_x(\eta^2+\tilde{h}^2)]$. For this to be much larger than 1, one needs

$$\frac{\eta}{\eta^2+\tilde{h}^2} \gg \frac{c\kappa_x}{\omega_c} = \frac{c}{v_s}\frac{\Delta\omega}{\omega_c}, \tag{26}$$

or $\Delta\omega/\omega_c \ll [v_s/(2c\tilde{h})]$, where we already used the maximum value $1/(2\tilde{h})$ of the function of η on the left hand side (lhs) in (26). For the standard parameters, we find $\Delta\omega/\omega_c \ll 1.66\times 10^{-9}$. When operating at ω_c in the GHz regime, this means that the correlation function essentially vanishes for $\Delta\omega$ larger than a few Hertz and thus bears no more information for the measurement of the position-dependent brightness temperature.

Another way of seeing this is to observe that (26) limits the integration range for η: The lhs of (26) is a function that starts at 0 for $\eta = 0$, increases linearly, reaches a maximum of $1/2\tilde{h}$ at $\eta = \tilde{h}$, and decays as $1/\eta$ for large η. Condition (26) then limits the integration range of η to an interval $\eta_1 \le \eta \le \eta_2$, with

$$\eta_{1,2} = \frac{1 \pm \sqrt{1 - 4\delta^2 \tilde{h}^2}}{2\delta} \equiv \eta_{1,2}(\kappa), \tag{27}$$

where $\delta \equiv c\Delta\omega/(v_s\omega_c) = c\kappa_x/\omega_c = c\kappa/(\omega_c\Delta r) = \chi\kappa$, $\kappa \equiv \kappa_x\Delta r$, and $\chi = c/(\omega_c\Delta r) \ll 1$ (see Sec. I and Fig. 2). A finite real integration range exists only for $\delta < 1/(2\tilde{h})$, equivalent to $\kappa < \frac{\omega_c\Delta r}{2c\tilde{h}} \equiv \kappa_{\rm Max}$. For a given η, we have $\kappa \le \kappa_{\max}(\eta) \equiv \frac{\omega_c\Delta r}{c}\frac{\eta}{\eta^2+\tilde{h}^2} \le \kappa_{\rm Max}$. A finite minimal value of κ can be deduced from a maximum desired snapshot size in the x-direction. Also the requirement $\tau < h/v_s$ may provide a lower bound of the relevant values of κ because it leads to the smallest resolvable frequency and thus also to the smallest resolvable $\Delta\omega$: $\Delta\omega > 2\pi/\tau \Rightarrow \kappa = \Delta r\Delta\omega/v_s > \Delta r\frac{2\pi}{\tau v_s} \equiv \kappa_{\min}$.

Because the contributions from areas outside the allowed range $\eta_1 \le \eta \le \eta_2$ (or, correspondingly, for negative η, $-\eta_2 \le \eta \le -\eta_1$) are exponentially suppressed, we can limit the integration range of η to that interval for a given κ_x and replace the integral kernel by its approximate form, Eq. (B5), extended to $\beta < 0$ by (B1), which yields

$$K(\alpha, \beta) \simeq \sqrt{\frac{2\pi}{|\beta|}} e^{\mathrm{sign}(\beta) i\frac{\pi}{4}} e^{-i\beta} \tag{28}$$

in the allowed range and zero elsewhere. After the substitution $\zeta = \eta/\sqrt{\eta^2 + \tilde{h}^2}$, the result for C_{ii} can be written as

$$C_{ii}(\mathbf{r}_1, \mathbf{r}_1 + \Delta r\hat{e}_y, \kappa, \tilde{k}_c) \simeq \sqrt{2\pi}\frac{K_6 e^{-i\kappa\tilde{x}_0}}{\sqrt{|\tilde{k}_c|}} \int_{-\infty}^{\infty} d\zeta F(\kappa, \zeta, \tilde{k}_c) e^{-i\tilde{k}_c\zeta}, \tag{29}$$

$$F(\kappa, \zeta, \tilde{k}_c) = \{e^{i\,\mathrm{sign}(\tilde{k}_c)\pi/4} w[\zeta_1(\kappa), \zeta_2(\kappa), \zeta] + e^{-i\,\mathrm{sign}(\tilde{k}_c)\pi/4} w[-\zeta_2(\kappa), -\zeta_1(\kappa), \zeta]\} \times \tilde{T}\left(\kappa, \frac{\zeta\tilde{h}}{\sqrt{1-\zeta^2}}\right) \frac{1}{\sqrt{|\zeta|}(1-\zeta^2)}, \tag{30}$$

where $\tilde{T}(\kappa, \eta) \equiv \tilde{T}_{0,\eta\Delta r}(\kappa_x)$ (with $\kappa = \kappa_x\Delta r$, $\tilde{x}_0 = x_0/\Delta r$) and $w(\zeta_1, \zeta_2, \zeta)$ is a window function equal to one for $\zeta_1 \le \zeta \le \zeta_2$ and zero elsewhere. The window functions translate, in a straight-forward fashion, the integration range for η into an integration range for ζ. By definition, ζ ranges from $-1, \ldots, 1$. So ζ_1, ζ_2 lies within this interval, $-1 \le \zeta_1, \zeta_2 \le 1$, and the window functions take care of restricting the argument ζ of the integrand to the intervals $\pm[\zeta_1, \zeta_2]$. We replaced ω_1, ω_2 by the equivalent information $\kappa \equiv \kappa_x\Delta r$ (related to $\Delta\omega$) and $\tilde{k}_c = \Delta r\omega_c/c$ (related to ω_c), and consider $i = j$ only. Given Eq. (29), it is tempting to try to recover $F(\kappa, \zeta, \tilde{k}_c)$ by Fourier transform. However, the $\mathrm{sign}(\tilde{k}_c)$ functions that appear in $F(\kappa, \zeta, \tilde{k}_c)$ prevent (29) from being a simple Fourier integral. Moreover, from the measured data, we only have C_{ij}^F, the filtered version of C_{ij}, that is restricted to a frequency range $\omega_1, \omega_2 \in \pm[\omega_0 - \pi B, \omega_0 + \pi B]$, where B is the bandwidth (20 MHz in SMOS for the L-band). We assume here, for simplicity, a Gaussian filter and the same filter for both antennas. For a real filter response function $A(t)$, its Fourier transform must satisfy $A(\omega) = A^*(-\omega)$. When also taking $A(\omega)$ as real, we can write it as

$$A(\omega) = [G(\omega; -\omega_0, b) + G(\omega; \omega_0, b)]\sqrt{b}\pi^{1/4}, \tag{31}$$

where $G(\omega; \omega_0, b) = \exp[-(\omega - \omega_0)^2/(2b^2)]/(\sqrt{2\pi}b)$ is a normalized Gaussian centered at ω_0 with the standard deviation $b \equiv 2\pi B$. The factor $\sqrt{b}\pi^{1/4}$ assures that $\omega_0 \gg b$, $A(\omega)$ is normalized according to $\int_{-\infty}^{\infty} |A(\omega)|^2 d\omega = 1$. Under the same condition, we have

$$C_{ii}^F(\mathbf{r}_1, \mathbf{r}_2, \kappa, \tilde{k}_c) = C_{ii}(\mathbf{r}_1, \mathbf{r}_2, \kappa, \tilde{k}_c) A(\omega_1) A^*(\omega_2), \tag{32}$$

$$A(\omega_1)A^*(\omega_2) = \frac{1}{2}\left(G\left(\tilde{k}_c; \tilde{k}_{c0}, \frac{\tilde{b}}{\sqrt{2}}\right) + G\left(\tilde{k}_c; -\tilde{k}_{c0}, \frac{\tilde{b}}{\sqrt{2}}\right)\right), \tag{33}$$

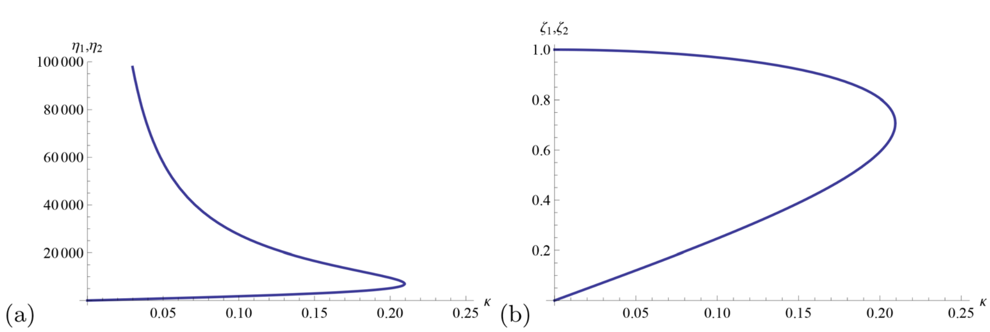

FIG. 2. Effectively contributing integration region as a function of $\kappa = \kappa_x\Delta r$ in terms of (a) η and (b) ζ. Only the area in the xy-plane between the two curves, $\eta_1 \le \eta \le \eta_2$, and, correspondingly, for ζ, contributes effectively to the correlation function for a given value of κ. The two curves join at $\kappa_{\rm Max} \simeq 0.21$ (for the numerical value for standard parameters, see Sec. I). Only the region with $\kappa, \eta \ge 0$ is shown; three more regions contribute in the other three quadrants, and the boundaries are obtained by reflecting the graph at the η-axes and κ-axes. The integration region translates directly into the area "seen" by the satellite in the y-direction for a given wave vector κ in the x-direction. For $\kappa \to 0$, the integration region is, in reality, cut off by the size of the Earth, and the smallest value of κ is determined by the desired size of the snapshot or the maximum time $\tau < h/v_s$.

where $\tilde{k}_{c0} = \Delta r\omega_0/c = 1/\chi \simeq 2932.55$, and $\tilde{b} = \Delta r b/c \simeq 41.89$. This contains the approximation of only using the "diagonal" terms in the product of $A(\omega_1)A^*(\omega_2)$, i.e., the ones with $\mathrm{sign}(\omega_1) = \mathrm{sign}(\omega_2)$, which is justified because $\Delta\omega \ll b \ll \omega_0$. The Fourier transform of C^F_{ii} with respect to $\tilde{k}_c$ (denoted by $\mathcal{F}_{\tilde{k}_c\to\zeta}$) gives a convolution product between the FT of the Gaussians [which is $(\sqrt{2}/\tilde{b})G(\zeta;0,\sqrt{2}/\tilde{b})e^{\pm i\tilde{k}_{c0}\zeta}$] and $F(\kappa,\zeta,\tilde{k}_c)$, and leads to

$$\mathcal{F}_{\tilde{k}_c\to\zeta}\left[C^F_{ii}(\mathbf{r}_1,\mathbf{r}_1+\Delta r\hat{e}_y,\kappa,\tilde{k}_c)\sqrt{\frac{|\tilde{k}_c|}{2\pi}}\frac{e^{i\kappa_x x_0}}{K_6}\right]$$
$$=\frac{\sqrt{2}}{\tilde{b}}\sum_{\sigma=\pm}\left[G\left(\zeta;0,\frac{\sqrt{2}}{\tilde{b}}\right)\cos\left(\tilde{k}_{c_0}\zeta+\sigma\frac{\pi}{4}\right)\right]$$
$$\star\left\{w[\zeta_1(\kappa),\zeta_2(\kappa),\sigma\zeta]\tilde{T}\left(\kappa,\frac{\zeta\tilde{h}}{\sqrt{1-\zeta^2}}\right)\frac{1}{\sqrt{|\zeta|}(1-\zeta^2)}\right\}, \tag{34}$$

where we used that the sign of $\tilde{k}_{c0}$ in (32) determines the one of $\tilde{k}_c$ in (30). Thus, we get back the original function $\tilde{T}\left(\kappa,\frac{\zeta\tilde{h}}{\sqrt{1-\zeta^2}}\right)=\tilde{T}(\kappa,\eta)$, cut by the two window functions and multiplied with $1/[\sqrt{\zeta}(1-\zeta^2)]$, convoluted with the product of a Gaussian of width $\sqrt{2}/\tilde{b}$ and a rapidly oscillating cosine function. The factor $1/[\sqrt{\zeta}(1-\zeta^2)]$ can be tracked back to the change of variables from η to ζ and will distort the image at the nadir and at infinity. Sources at positive or negative η contribute differently due to the different sign of the $\pi/4$ phase shift. This already arises in (28) due to the different phase shift in the asymptotics of the Struve functions for negative or positive arguments and leads to the sum over $\sigma=\pm$. In general, an exact inversion cannot simply be done by Fourier transform but needs a numerical approach. Nevertheless, we can arrive at an estimation of the resolution by considering a single point source because then only one of the two terms in the sum over σ in (34) contributes, and the factor $1/[\sqrt{\zeta}(1-\zeta^2)]$ becomes a simple numerical factor given by the position of the source.

B. Single point source and geometric resolution

1. Correlation function and reconstructed image

Let the point source be at position $x''=0, y''=\eta_s\Delta r$ and with polarization i, where η_s is situated in the allowed range $0\le\eta_1(\kappa)\le\eta_s\le\eta_2(\kappa)$ for some κ in the desired range up to the largest considered $\kappa=2\pi/p_x$, where p_x is the pixel size. We thus have

$$T(\mathbf{r}'')=T_0\delta(x'')\delta(y''-\eta_s\Delta r)\Delta r^2\,. \tag{35}$$

By following the above approximate analytical formalism, we show, in Appendix A–D, that the reconstructed profile is given by

$$T_{\mathrm{rec}}(x,y)=\frac{T_0\sqrt{\zeta_s}(1-\zeta_s^2)}{\sqrt{2}\pi^{3/2}\chi\tilde{h}^2}e^{-(\zeta-\zeta_s)^2\tilde{b}^2/4}$$
$$\times\cos\left[\tilde{k}_{c0}(\zeta-\zeta_s)+\frac{\pi}{4}\right]\mathrm{sinc}[\kappa_{\max}(\zeta_s)\tilde{x}/\pi]\,, \tag{36}$$

where $\zeta_s=\eta_s/\sqrt{\eta_s^2+\tilde{h}^2}$, $\kappa_{\max}(\zeta_s)\equiv\zeta_s\sqrt{1-\zeta_s^2}/(\chi\tilde{h})$, $\tilde{x}=x/\Delta r$ and $\mathrm{sinc}(x)\equiv\sin(\pi x)/(\pi x)$.

2. Geometric resolution

We see that the reconstructed image of the point source is a series of narrow peaks spaced by the inverse of $\tilde{k}_{c_0}$ due to the rapidly oscillating cos-function, under an approximate Gaussian in the y-direction centered at the position of the source with a width in η given by $\Delta\eta=\sqrt{2}\sqrt{\eta_s^2+\tilde{h}^2}/\tilde{b}\ge\sqrt{2}\tilde{h}/\tilde{b}=hc/[(\Delta r)^2\sqrt{2}\pi B]$. It reminds one of a diffraction image from a double slit, even though the envelope is a sinc-function not Gaussian. Nevertheless, we adapt the definition of resolution from that example, namely, that the best resolution is obtained from the smallest shift that makes a peak move into the next trough. This leads to

$$\tilde{k}_{c_0}\frac{\partial}{\partial\eta}\frac{\eta}{\sqrt{\eta^2+\tilde{h}^2}}\bigg|_{\eta=\eta_s}\Delta\eta\simeq\pi\,, \tag{37}$$

hence, $\Delta y=\Delta r\pi(\eta_s^2+\tilde{h}^2)^{3/2}/(\tilde{k}_{c_0}\tilde{h}^2)$. For $y\simeq h$, this is on the order of $2\sqrt{2}\pi hc/(\Delta r\omega_c)=\chi h$. The numerical value for the standard parameters gives $\Delta y\simeq 2.1$ km, i.e., a resolution on the order of a kilo-meter. However, for actually achieving this resolution for an extended source, one has to face two issues: (i) The reconstructed point-source image should be brought as close as possible to a single narrow peak, and (ii) one has to deal with the different phases from sources at a positive or negative η. The first issue can be addressed by superposing correlation functions from pairs of antennas at different separations and/or by changing the considered central frequency. This shifts the pattern of peaks due to the cos function, and one can engineer a rather narrow central peak (see Ref. 14 for details). The second issue should be absent in a numerically exact inversion of the integral kernel. The Gaussian envelope has a width of $hc/(\sqrt{2}\pi B\Delta r)$, given by the inverse bandwidth, which is much larger than the width of a single peak, namely, by a factor of $\omega_c/(4\pi B)\simeq 35$ for the standard parameters.

The resolution in the x-direction follows from the effective wave vector $\kappa_{\max}$ in the sinc function. It depends on the position of the source and reaches its maximum possible value of κ_{Max} for $\eta_s=\tilde{h}$ (i.e., $y_s=h$). The inverse of κ_{Max} therefore gives the best possible resolution in the x-direction

$$\Delta x\ge\frac{\Delta r}{\kappa_{\mathrm{Max}}}=\frac{2hc}{\omega_c\Delta r}\,. \tag{38}$$

We conclude that, in both the x- and the y-direction, one can expect a geometric resolution on the order of $h\chi=c/(\Delta r\omega_c)$ for sources close to $y=h$. For sources close to $y=0$, $\kappa(\eta_s)$ goes to zero $\propto\eta_s$, whereas, for larger y_s, the decay of $\kappa(\eta_s)$ is $\propto 1/\eta_s$. The geometric resolution in the x-direction deteriorates correspondingly. The resolution in the y-direction, however, depends only weakly on the source position, as $(\eta_s^2+\tilde{h}^2)^{3/2}/(\tilde{k}_c\tilde{h}^2)$ increases monotonically from $\tilde{h}$ at $y_s=0$ to $2\sqrt{2}$ at $y_s=h$ and keeps growing slowly beyond $y_s=h$. The resolution in the y-direction is what would also be expected from a standard aperture-synthesization approach. It should be kept in mind, however, that the procedure here is very different, and it is rather remarkable that correlating electric fields at two different frequencies can lead to a resolution given by the central frequency.

The definition of $\kappa_{\max}$ is based on the request that the stationary phase approximation (SPA) should hold in the regime $\beta \gg \alpha$. In practice, the SPA is almost always better than expected, such that, in the end, the result $h\chi$ might be a conservative estimate of the geometric resolution.

V. RADIOMETRIC RESOLUTION

Besides the geometric resolution, the radiometric resolution (RR), i.e., the smallest difference in temperature that the system can measure for a given pixel, is the most important characteristic of the satellite imaging system (one might also call this radiometric uncertainty). Here we calculate the RR for the idealized situations of a single point source considered above and for a uniform temperature field in the positive half-plane $y>0$.

A. Fluctuations of the reconstructed temperature profiles

The idea behind the calculation of RR is that the electric field measurements yield random values whose fluctuations and correlations reflect the thermal nature of the radiation field. Thus, if one repeated the measurement many times with the same field T(x,y), then one would obtain different correlation functions in each run, and thus, after inverting the linear relationship between C_{ij} and $T(x, y)$, also different reconstructed $T(x, y)$ (called $T_{\rm rec}$ in the following) in each run. The (relative) RR is then defined as the standard deviation $\sigma[T_{\rm rec}(x,y)]$ divided by the average $T_{\rm rec}(x,y)$ for a given position x, y. In general, it will vary as the function of x, y, and also depends on the temperatures at all positions, a behavior well known from standard spatial aperture synthesis. In reality, things still become a bit more complicated because the measured signal is a superposition of the e.m. field emitted by the antenna itself (at temperature T_a), and the radiated field from the surface of the Earth. However, these fields are uncorrelated, and their averaged squares just add. For simplicity, we ignore the noise contribution of the antennas in this first analysis, which amounts to calculating the lower bounds of $\sigma(T_{\rm rec})$.

The starting point of the calculation is the assumption that the current fluctuations $\mathbf{j}(\mathbf{r}'',t)$, which are at the origin of the radiated thermal field, are described by a random Gaussian process, both in time and space (see Sec. II). This immediately implies, also that the temporal FT $\tilde{\mathbf{j}}(\mathbf{r}'',\omega')$ of the current fluctuations is a Gaussian process, now over space and frequency. Finally, the connection between $\tilde{\mathbf{j}}(\mathbf{r}'',\omega')$ and $\tilde{E}_{\mathbf{r}_1}(\omega_1)$ is linear, which implies that $\tilde{E}_{\mathbf{r}_1}(\omega_1)$ is a Gaussian process over $\mathbf{r}_1$ and ω_1. By the nature of this variable, it is a complex Gaussian process. One easily shows that the average of $\tilde{E}_{\mathbf{r}_1}(\omega_1)$ equals zero (if the average of all current components is zero, which must be true at thermal equilibrium). The correlation function C_{ij} is the (complex) covariance matrix of this Gaussian process, and all higher correlations can be expressed in terms of it.

To assess the fluctuations of $T_{\rm rec}$, we first define a product of Fourier coefficients of $\mathbf{E}$ from a single run (denoted by a $\hat{}$),

$$\hat{C}(\mathbf{r}_1,\mathbf{r}_2,\kappa,\tilde{k}_c) \equiv \hat{C}_{zz}(\mathbf{r}_1,\mathbf{r}_2,\omega_1,\omega_2) \equiv \hat{\tilde{E}}_{z,\mathbf{r}_1}(\omega_1)\hat{\tilde{E}}^*_{z,\mathbf{r}_2}(\omega_2), \tag{39}$$

$$= \frac{1}{2\pi}\int dt_1 \int dt_2 \hat{E}_{z,\mathbf{r}_1}(t_1)\hat{E}_{z,\mathbf{r}_2}(t_2)e^{-i\omega_1 t_1 + i\omega_2 t_2}, \tag{40}$$

and its corresponding filtered version $\hat{C}^F(\mathbf{r}_1,\mathbf{r}_2,\kappa,\tilde{k}_c) = \hat{C}(\mathbf{r}_1,\mathbf{r}_2,\kappa,\tilde{k}_c)A(\omega_1)A^*(\omega_2)$ (with ω_1,ω_2 expressed in terms of $\kappa,\tilde{k}_c$).

The fluctuations of $T_{\rm rec}(x,y)$ are defined as $\Delta T_{\rm rec}(x,y) \equiv \langle T_{\rm rec}(x,y)^2\rangle - \langle T_{\rm rec}(x,y)\rangle^2$, where the average is over the thermal ensemble. With $T_{\rm rec}(x,y)$ from (C4), one finds

$$\begin{aligned}\Delta T_{\rm rec}(x,y) = &\frac{1}{K_6^2(2\pi)^3\Delta r^2}\int d\kappa_1\, d\kappa_2\, d\tilde{k}_{c1}\, d\tilde{k}_{c2} \\ &\times \sqrt{|\tilde{k}_{c1}\tilde{k}_{c2}|}e^{-i(\kappa_1-\kappa_2)(\tilde{x}-\tilde{x}_0)}e^{i(\tilde{k}_{c1}-\tilde{k}_{c2})\zeta} \\ &\times \Big[\langle \hat{C}^F(\mathbf{r}_1,\mathbf{r}_2,\kappa_1,\tilde{k}_{c1})\hat{C}^{F*}(\mathbf{r}_1,\mathbf{r}_2,\kappa_2,\tilde{k}_{c2})\rangle \\ &-\langle \hat{C}^F(\mathbf{r}_1,\mathbf{r}_2,\kappa_1,\tilde{k}_{c1})\rangle\langle \hat{C}^{F*}(\mathbf{r}_1,\mathbf{r}_2,\kappa_2,\tilde{k}_{c2})\rangle\Big].\end{aligned} \tag{41}$$

In Appendix A 2, we show that, in the narrow frequency intervals considered, the correlation function contained within the large parenthesis of (C4) can be written as

$$C_{zz}^F(\mathbf{r}_1,\mathbf{r}_1,\kappa_{13},\tilde{k}_{c13})C_{zz}^{F*}(\mathbf{r}_2,\mathbf{r}_2,\kappa_{24},\tilde{k}_{c24}), \tag{42}$$

with $\kappa_{ij} = \Delta r(\omega_j - \omega_i)/v_s$, $\tilde{k}_{cij} = \Delta r(\omega_i+\omega_j)/(2c)\,\forall i,j$, and the single-point function

$$C_{zz}(\mathbf{r}_1,\mathbf{r}_1,\kappa,\tilde{k}) = K_6 e^{-i\kappa\tilde{x}_0}\pi\int d\eta' \frac{\tilde{T}_{0,\eta'}(\kappa)e^{-|\kappa|\sqrt{\eta'^2+\tilde{h}^2}}}{\sqrt{\eta'^2+\tilde{h}^2}}. \tag{43}$$

We calculate $\Delta T_{\rm rec}$ for the single point source considered in Sec. IV B at the position of the source, i.e., $\Delta T_{\rm rec}(x_s,y_s) = [T_{\rm rec}(x_s,y_s)^2] - [T_{\rm rec}(x_s,y_s)]^2$, and for a uniform temperature field.

B. Single point source

For the single point source at position $(0,y_s)$, the correlation function $C_{zz}(\mathbf{r}_1,\mathbf{r}_1,\kappa,\tilde{k})$ becomes [see Eq. (C1)]

$$C_{zz}(\mathbf{r}_1,\mathbf{r}_1,\kappa,\tilde{k}) = K_6\sqrt{\frac{\pi}{2}}T_0 e^{-i\kappa\tilde{x}_0}\frac{e^{-|\kappa|\sqrt{\eta_s^2+\tilde{h}^2}}}{\sqrt{\eta_s^2+\tilde{h}^2}}. \tag{44}$$

Insert this into Eq. (41) to find

$$\Delta T_{\rm rec}(0,y_s) = \frac{T_0^2}{16\pi^2}\int d\kappa_{12}d\kappa_{34}d\tilde{k}_{c12}d\tilde{k}_{34}\sqrt{|\tilde{k}_{c12}\tilde{k}_{c34}|} \times \frac{e^{-(|\kappa_{13}|+|\kappa_{24}|)\sqrt{\eta_s^2+\tilde{h}^2}}}{\eta_s^2+\tilde{h}^2} \times \left[G\left(\tilde{k}_{c13};\tilde{k}_{c0},\frac{\tilde{b}}{\sqrt{2}}\right)+G\left(\tilde{k}_{c13};-\tilde{k}_{c0},\frac{\tilde{b}}{\sqrt{2}}\right)\right] \times \left[G\left(\tilde{k}_{c24};\tilde{k}_{c0},\frac{\tilde{b}}{\sqrt{2}}\right)+G\left(\tilde{k}_{c24};-\tilde{k}_{c0},\frac{\tilde{b}}{\sqrt{2}}\right)\right] \times e^{i(\kappa_{12}-\kappa_{34}-\kappa_{13}+\kappa_{24})\tilde{x}_0+i(\tilde{k}_{c12}-\tilde{k}_{c34})\zeta_s}. \tag{45}$$

We change integration variables to $\kappa_{13},\tilde{k}_{c13},\kappa_{24},\tilde{k}_{c24}$. The Jacobian is 1. In the product of the Gaussians, only the diagonal terms (i.e., with the same signs in front of $\tilde{k}_{c0}$) contribute in the relevant regime $\tilde{k}_{c0}\gg\tilde{b}$, as for the opposite signs, $\tilde{k}_{c12}\simeq\tilde{k}_{c34}\simeq 0$. Finally, we approximate

$$\tilde{k}_{c12}=\tilde{k}_{c34}\simeq\tilde{k}_{c0} \tag{46}$$

and pull that factor out from the integral, which is permissible for all ranges of the variables for which the product of Gaussians is non-negligible. The integrals can then be performed, and we find, for the standard deviation, $\sigma[T_{\rm rec}(0,y_s)] \equiv \sqrt{\Delta[T_{\rm rec}(0,y_s)]}$

$$\sigma[T_{\rm rec}(0,y_s)] = \frac{T_0}{\sqrt{2\pi}}\frac{|\tilde{k}_{c0}|^{1/2}}{\eta_s^2+\tilde{h}^2+\frac{\beta^2\zeta_s^2}{4}} \simeq \frac{T_0}{\sqrt{2\pi}}\frac{|\tilde{k}_{c0}|^{1/2}}{\eta_s^2+\tilde{h}^2}, \tag{47}$$

where, in the last step, we used $\tilde{h}\gg 1$ and $\beta\zeta_s\ll 1$ (where, once more, $\beta=v_s/c$).

From (36), we find

$$T_{\rm rec}(0,y_s) = \frac{T_0\sqrt{\eta_s}}{2\pi^{3/2}\chi(\eta_s^2+\tilde{h}^2)^{5/4}}. \tag{48}$$

When combined with (47), we obtain the relative RR

$$\frac{\sigma[T_{\rm rec}(0,y_s)]}{T_{\rm rec}(0,y_s)} = \sqrt{\frac{2\pi\chi}{\eta_S}}(\eta_s^2+\tilde{h}^2)^{1/4}. \tag{49}$$

For $\eta_s=\tilde{h}$, the relative RR is on the order of 0.055, which corresponds at $T=300$ K to $\sigma[T_{\rm rec}(0,h)]\simeq 16.5$ K.

When judging this value, it should be kept in mind that it is based on expressing the fluctuations $\sigma(T_{\rm rec})$ in units of the reconstructed temperature, whose approximate analytical form (48) is not an unbiased estimate of T_0 itself due to the additional geometrical factors $\propto\sqrt{\eta_s}/\chi(\eta_s^2+\tilde{h}^2)^{5/4}$ and the constant $1/2\pi^{3/2}$. From standard radiometry, one is used to obtain an RR that improves as $1/\sqrt{t_{\rm mes}}$ with the total measurement time, a fact that can be attributed to obtaining a number of independent samples that scales $\propto t_{\rm mes}$. For Fourier-correlation imaging, however, no such improvement with $t_{\rm mes}$ is possible because all measured fields for given times are already used for calculating the Fourier transform (see also the discussion in Sec. VI A).

C. Uniform temperature field

We now look at the second standard situation commonly considered for the determination of the radiometric resolution, namely, a field of constant temperature. More precisely, we consider

$$T(x,y) = \begin{cases} T_0 & 0\le y\le\hat{y} \\ 0 & \text{else.}\end{cases} \tag{50}$$

The restriction to sources in the upper plane is because we still want to use Eq. (C4) for calculating the reconstructed temperature profile. The cutoff $\hat{y}$ arises physically from the size of the Earth and prevents a divergence of the correlation function.

From (13) we obtain

$$\tilde{T}(\kappa_x,\eta) = \begin{cases} \sqrt{2\pi}\delta(\kappa_x)T_0 & 0\le y\le\hat{y} \\ 0 & \text{else.}\end{cases} \tag{51}$$

The correlation function (43) becomes

$$C_{ii}(\mathbf{r}_1,\mathbf{r}_1,\kappa,\tilde{k}_c) = K_6\sqrt{2}\pi^{3/2}T_0e^{-i\kappa\tilde{x}_0}\delta(\kappa)\Delta r\int_0^{\hat{\eta}}\frac{d\eta}{\sqrt{\eta^2+\tilde{h}^2}}, \tag{52}$$

$$= K_6\sqrt{2}\pi^{3/2}T_0e^{-i\kappa\tilde{x}_0}\delta(\kappa)\Delta r\ln\left(\frac{\hat{\eta}+\sqrt{\hat{\eta}^2+\tilde{h}^2}}{\tilde{h}}\right), \tag{53}$$

with $\hat{\eta}\equiv\hat{y}/\Delta r$. For $\hat{y}=R_E\simeq 6370$ km, the radius of the Earth, and $\Delta r=100$ m, $\hat{\eta}=63\,700$. We see that here, the correlation function is perfectly diagonal in frequency, which reflects the lack of structure of the temperature field in the x-direction. Hence, we can set everywhere $\kappa=0$, which greatly simplifies the analysis. The cutoff $\hat{\eta}$ in Eq. (52) prevents a logarithmic divergence that arises from $1/\sqrt{\eta^2+\tilde{h}^2}\sim 1/\eta$ for $\eta\to\infty$. Equation (52) can be extended to a temperature field that is uniform everywhere, from $-\hat{y}$ to $\hat{y}$. In this case, the ζ-integral starts at $-1+\epsilon$ rather than at 0. However, in this situation, we cannot use Eq. (C4) anymore because it is valid only for sources at positive y (see the discussion after (34)).

Equation (52), when inserted into (41), and with the same change of integration variables and approximation in (46), leads to

$$\sigma[T_{\rm rec}(0,y)] = \frac{T_0}{\sqrt{2}}\sqrt{|\tilde{k}_{c0}|}\ln\left(\frac{\hat{\eta}+\sqrt{\hat{\eta}^2+\tilde{h}^2}}{\tilde{h}}\right). \tag{54}$$

The reconstructed temperature field [Eq. (C5)] is given by

$$T_{\rm rec}(x,y) = \frac{T_0}{\sqrt{2\pi}}\int_0^{\hat{\zeta}}d\zeta'\frac{e^{-\tilde{b}^2(\zeta-\zeta')^2/4}}{\sqrt{|\zeta'|}(1-\zeta'^2)}\cos\left[\tilde{k}_{c0}(\zeta-\zeta')+\frac{\pi}{4}\right]. \tag{55}$$

Unfortunately, no closed analytical form could be found for the remaining integral, and even a numerical evaluation is not straight-forward because the Gaussian yields a very narrow peak, broader, however, than the period of the cos-function. But we can get an estimate of $T_{\rm rec}$ by replacing the Gaussian (normalized to an integral equal to 1), with a rectangular peak of width $a\sigma$ and height $1/(a\sigma)$ centered, as the Gaussian, at ζ. Here, $\sigma=\sqrt{2}/\tilde{b}$, and a is a parameter of order 1. This gives

$$T_{\rm rec}(x,y)=\frac{T_0}{a}\int_{\max(0,\zeta-a\sigma/2)}^{\min(\hat{\zeta},\zeta+a\sigma/2)}d\zeta'\,\frac{\cos\left[\tilde{k}_{c0}(\zeta-\zeta')+\frac{\pi}{4}\right]}{\sqrt{|\zeta'|}(1-\zeta'^2)}\,. \tag{56}$$

A numerical evaluation of the integral is now relatively straight-forward and shows a slowly varying $T_{\rm rec}(0,y)$ as a function of ζ in the interval $\zeta\in[a\sigma/2,\hat{\zeta}-a\sigma/2]$, whereas, outside this interval, it oscillates rapidly. The slow variation arises from the factor $\sqrt{|\zeta'|}(1-\zeta'^2)$, which distorts this approximately reconstructed image. By pulling out this slowly varying factor to get an analytical estimate of the order of magnitude of $T_{\rm rec}(x,y)$, we are led to

$$T_{\rm rec}(x,y)\simeq T_0\frac{\sqrt{2}}{a\tilde{k}_{c0}}\frac{1}{\sqrt{|\zeta|}(1-\zeta^2)}\sin\left(\frac{a\tilde{k}_{c0}}{\sqrt{2}\tilde{b}}\right) \tag{57}$$

for $\zeta\in[a\sigma/2,\hat{\zeta}-a\sigma/2]$. Hence, in this interval and apart from the distorting factor $1/\sqrt{|\zeta|}(1-\zeta^2)$ identified previously, we recover a constant temperature field. The value of the reconstructed temperature depends on the precise value of a as well as the ratio $\tilde{k}_{c0}/\tilde{b}$. Outside the mentioned interval, $T_{\rm rec}(x,y)$ oscillates again as a function of ζ, which can be understood from the fact that the box is cut off when ζ gets within a distance $a\sigma/2$ of 0 or $\hat{\zeta}$. The sought-after order of magnitude can be estimated from the maximum value of (57) as a function of a. As for standard parameters $\tilde{k}_{c0}/\tilde{b}\simeq 70$, we can bound the sin-function by one (while still having $a\sim 1$), in which case, we obtain $T_{\rm rec}(x,y)\simeq T_0/\tilde{k}_{c0}=T_0\chi$ in the mentioned ζ-interval. With all this, and approximating $\sqrt{\tilde{h}^2+\hat{\eta}^2}\simeq\hat{\eta}$ in the logarithm in (54), we find the order of magnitude $\sigma[T_{\rm rec}(x,y)]/T_{\rm rec}(x,y)\sim\ln(2\hat{\eta}/\tilde{h})/\chi^{3/2}$. For $\zeta\sim 1$, this is on the order of $\sim 10^5$ for standard parameters, i.e., a catastrophically large uncertainty. A small value of $\sigma[T_{\rm rec}(x,y)]/T_{\rm rec}(x,y)$ is possible only if $\sqrt{|\zeta|}(1-\zeta^2)$ is very small, but, apart from the fact that one should not rely on this image-distorting factor, it could only be sufficiently small for y unrealistically close to the nadir.

If one traces the difference back to the single-point source, one realizes that, although $\sigma(T_{\rm rec})$ scales in both cases as $1/\sqrt{\chi}$, the difference comes from $T_{\rm rec}$ itself: for the single point source, it is on the order of $1/\chi$ but, for uniform T in the upper half plane of order χ, which explains a factor $1/\chi^2$ worse relative RR for the latter compared with the former. The factor $1/\chi$ in the single-point $T_{\rm rec}$ arises from the cutoff of the κ integral: $\kappa_{\rm Max}$ scales as $1/\chi$, and, for $x=0$, the κ-integral in (C4) just gives a factor $2\kappa_{\rm Max}\sim 1/\chi$ because the correlation-function is independent of κ in this case. However, for a constant temperature in the upper half-plane, the cutoffs $\kappa_{\rm Max}$ do not play a role because the $\delta(\kappa)$-function only picks up $\kappa=0$. This leads to the loss of one factor, $1/\chi$, in $T_{\rm rec}$. The second one comes from the integration over ζ' in (55): the rapidly oscillating cos-function leads to a factor $1/\tilde{k}_{c0}=\chi$, whereas, for the point-source, only a single point $\zeta=\zeta_s$ contributes, such that the cosine is on the order of one. One might wonder whether the relative radiometric resolution should be calculated by using, as a reference, the reconstructed $T(x,y)$, if that is off by a factor of χ. Only a numerical approach can tell.

In light of the RR of standard radiometers that typically scales as $\sigma(T)\propto 1/\sqrt{Bt_{\rm int}}$, where $t_{\rm int}$ is the integration time, the fact that $\sigma(T_{\rm rec})$ in Eqs. (47) and (54) is independent of the bandwidth is rather surprising. Formally, the disappearance of $\tilde{b}$ can be traced back to using the lowest order in the Laplace approximation of (45). The next order corrections are of the order $\tilde{b}$, such that $\sigma(T_{\rm rec})\to\sigma(T_{\rm rec})[1+\mathcal{O}(\tilde{b})]$. One expects the sign of the correction to be positive because the integrand is positive everywhere, and the lowest order approximation amounts to replacing the Gaussians by normalized Dirac-delta functions. Hence, for small but finite $\tilde{b}$, $\sigma(T_{\rm rec})$ is expected to increase with $\tilde{b}$, which is contrary to the behavior of standard radiometers. Standard radiometers are based on the van Cittert-Zernike theorem, which gives the reconstructed temperature field as a Fourier transform of the observed visibilities at a fixed frequency. Different frequencies at the source are uncorrelated, and the scaling of $\sigma(T_{\rm rec})/T_0\propto 1/\sqrt{Bt_{\rm int}}$ just reflects averaging over a number of independent measurements that scales $\propto B\,t_{\rm int}$. In FouCoIm, the information is in the correlation between different, very narrowly spaced Fourier components, and averaging over the central frequency does not lead to additional information (see also Sec. VI B). Therefore, a larger bandwidth does not improve the RR.

VI. NOISE REDUCTION

The bad signal-to-noise ratio for the radiometric resolution in the case of a uniform temperature field in the upper half plane makes it essential to consider measures that lead to a noise reduction and, in particular, averaging schemes.

A. Averaging over time

Instead of examining $T_{\rm rec}(x,y)$, for simplicity we consider here the fluctuations of the measured "single shot" correlation function $\hat{C}_{ij}$ directly. The first idea that comes to mind for reducing the fluctuations of $\hat{C}_{ij}$ is to average over the origin of the time interval from which we construct the Fourier transform. Note that this is very different from an ensemble that one would obtain by displacing the initial position $\mathbf{r}_i$. However, averaging over the origin of time only leads to an overall factor of

$$C^{\rm exp}(\mathbf{r}_1,\mathbf{r}_2,\omega_1,\omega_2)\equiv\int_{-\tau_a/2}^{\tau_a/2}dt\int dt_1\int dt_2\times E_{z,\mathbf{r}_1}(t_1+t)E_{z,\mathbf{r}_2}(t_2+t)e^{-i\omega_1 t_1+i\omega_2 t_2}, \tag{58}$$

$$= \mathrm{sinc}\left[(\omega_1 - \omega_2)\frac{\tau_a}{2\pi}\right]\hat{C}(\mathbf{r}_1, \mathbf{r}_2, \omega_1, \omega_2). \tag{59}$$

Hence, correlation functions calculated by transforming the measured fields by integrating with different starting points in time are not statistically independent, which renders this kind of averaging useless. Indeed, this is to be expected because all available data were already used. The situation improves only slightly if the FTs are calculated from a finite stretch of data (say, over a duration τ_F); then shifting the origin in time will include some new random data. For a satellite that is mapping the Earth rather than an infinitely extended plane, it is, in fact, mandatory to shift the origin of time every 0.28 s for standard parameters when a new pixel of size 2 km comes into view of the satellite, but this corresponds to analyzing a slightly new scenery. Most of the pixels are still the same, but still, for averaging purposes, we want to include only data that correspond to the same scenery. Hence, the averaging time τ_a should be smaller than the time for flying over one pixel, i.e., $\tau_a \lesssim 0.28$ s. With the time interval used for Fourier transformation of length $\tau_F \simeq 100$ s, we necessarily have $\tau_F \gg \tau_a$. It is then clear that we still essentially use the same data with the exception of some new data points at the edge of the time interval τ_F. Therefore, the obtained Fourier components are not statistically independent but rather highly correlated, and not much can be gained by averaging over time.

B. Additional frequency pairs

By using only a small frequency separation of width $\Delta\omega$ about the central frequency ω_c, which itself is allowed to vary over a large bandwidth, B seems to be a very wasteful use of all the pairs of frequency components $[\tilde{E}_{z,\mathbf{r}_1}(\omega_1), \tilde{E}_{z,\mathbf{r}_2}(\omega_2)]$. Can we use different measured correlations $\hat{C}(\mathbf{r}_1, \mathbf{r}_2, \omega_1, \omega_2)$ with sufficiently different $\omega_c = (\omega_1 + \omega_2)/2$ as independent data for improving the radiometric sensitivity? To answer this question, we need to calculate the covariance matrix V between two different correlators,

$$V \equiv \langle \hat{C}(\mathbf{r}_1, \mathbf{r}_2, \omega_1, \omega_2)\hat{C}^*(\mathbf{r}_1, \mathbf{r}_2, \omega_1', \omega_2')\rangle - \langle \hat{C}(\mathbf{r}_1, \mathbf{r}_2, \omega_1, \omega_2)\rangle\langle \hat{C}^*(\mathbf{r}_1, \mathbf{r}_2, \omega_1', \omega_2')\rangle, \tag{60}$$

as well as the pseudo-covariance matrix M,

$$M \equiv \langle \hat{C}(\mathbf{r}_1, \mathbf{r}_2, \omega_1, \omega_2)\hat{C}(\mathbf{r}_1, \mathbf{r}_2, \omega_1', \omega_2')\rangle - \langle \hat{C}(\mathbf{r}_1, \mathbf{r}_2, \omega_1, \omega_2)\rangle\langle \hat{C}(\mathbf{r}_1, \mathbf{r}_2, \omega_1', \omega_2')\rangle. \tag{61}$$

Both matrices together determine the statistical properties of the random process $\hat{C}(\mathbf{r}_1, \mathbf{r}_2, \omega_1, \omega_2)$. Note that, despite the fact that $E_{z,\mathbf{r}}(\omega)$ can be considered a circularly symmetric Gaussian process (see Appendix A–D) over $\mathbf{r}$ and ω in the narrow frequency band that we are interested in, the same is not true for $\hat{C}(\mathbf{r}_1, \mathbf{r}_2, \omega_1, \omega_2) - \langle \hat{C}(\mathbf{r}_1, \mathbf{r}_2, \omega_1, \omega_2)\rangle$ (which is not even Gaussian). We need to know whether both V and M essentially vanish for almost all pairs of pairs of frequencies, with the first pair (ω_1, ω_2) in a first region (notably, in the central narrow strip $S \equiv \omega_2 \in [\omega_1 - \Delta\omega, \omega_1 + \Delta\omega]$), and the second pair (ω_1', ω_2') in another region in the (ω_1, ω_2) plane that we may want to consider, whereas the correlation functions $C_{ij}(\mathbf{r}_1, \mathbf{r}_2, \omega_1, \omega_2)$ and $C_{ij}(\mathbf{r}_1, \mathbf{r}_2, \omega_1', \omega_2')$ themselves should still be non-zero. Such a situation would signal statistically independent non-vanishing correlation functions. However, we saw that only within a central narrow strip S (whose width is given by $\kappa_{\max}(\eta)$) in the $(\omega_1, \omega_2)-$ plane C_{ij} is non-zero and that, within this strip, all pairs of frequencies are used for obtaining a single profile $T(x, y)$. Hence, this is not a viable approach either. In Appendix D, we show the same thing once more rigorously.

C. Additional antennas

So far, we considered only two antennas. As mentioned before, to obtain a reconstructed single source image with a single peak, one may sum the correlated signals from several antenna pairs. It is to be expected that this will reduce $\sigma(T_{\mathrm{rec}})/T_{\mathrm{rec}}$, but we have to figure out how far two pairs of antennas have to be separated to essentially produce uncorrelated correlation functions. To answer this question, we have to generalize Eq. (60) to pairs of correlators at different points $\mathbf{r}_1', \mathbf{r}_2'$. We define

$$V_r \equiv \langle \hat{C}(\mathbf{r}_1, \mathbf{r}_2, \omega_1, \omega_2)\hat{C}^*(\mathbf{r}_3, \mathbf{r}_4, \omega_1, \omega_2)\rangle - \langle \hat{C}(\mathbf{r}_1, \mathbf{r}_2, \omega_1, \omega_2)\rangle\langle \hat{C}^*(\mathbf{r}_3, \mathbf{r}_4, \omega_1, \omega_2)\rangle, \tag{62}$$

where we take $\mathbf{r}_{i+2} = \mathbf{r}_i + \rho_i\hat{e}_y$ for $i = 1, 2$, i.e., the antennas in the second pair are shifted by distance ρ_i in the y-direction compared with the corresponding ones in the first pair. From (A14), we have

$$V_r = C(\mathbf{r}_1, \mathbf{r}_3, \omega_1, \omega_1)C(\mathbf{r}_4, \mathbf{r}_2, \omega_2, \omega_2)\,, \tag{63}$$

where, from (21) and (B6),

$$C(\mathbf{r}_1, \mathbf{r}_3, \omega_1, \omega_1) = K_6\int \frac{d\eta}{\sqrt{\eta^2 + \tilde{h}^2}} \times K\left(0, \frac{\rho_1\omega_1}{c}\frac{\eta}{\sqrt{\eta^2 + \tilde{h}^2}}\right)\tilde{T}(0, \eta), \tag{64}$$

$$= K_6\int \frac{d\zeta}{1 - \zeta^2}\left[J_0\left(\frac{\rho_1\omega_1\zeta}{c}\right) - iH_0\left(\frac{\rho_1\omega_1\zeta}{c}\right)\right]. \tag{65}$$

The corresponding result for $C(\mathbf{r}_4, \mathbf{r}_2, \omega_2, \omega_2)$ is obtained from the last line in (64) by replacing $\rho_1 \to \rho_2$. For the uniform temperature field in the upper half plane up to a cutoff $\hat{y}$ and also a cutoff of the same value in the x-direction, we have $T(0, \eta) = \hat{y}T_0/\pi$ for $0 \le y \le \hat{y}$. No closed form was found for the remaining integral over ζ, but a closed form is easily obtained if we neglect the slowly varying envelope $1/(1 - \zeta^2)$, which is legitimate for cutoffs $\hat{\eta}$ not too close to 1 and gives an idea on which length-scale V_r will vanish. By plotting the results of the integration, one finds that both the real and imaginary parts decay on a scale of $\rho_i\omega_0/c \sim 1$, where we have again used $\omega_1 \simeq \omega_2 \simeq \omega_0$. Hence, for the correlation functions of two pairs of antennas to decorrelate, it is enough that one antenna in one pair be at a distance on the order of $r \gtrsim c/\omega_0 = \lambda/2\pi$, i.e., on the order of the central wave-length λ with respect to at least one antenna of the other pair. For standard parameters, this is on the order of 10 cm when neglecting factors are on the order of 1 [the 2π helps, but, for the imaginary part of $C(\mathbf{r}_1, \mathbf{r}_2, \omega_1, \omega_1)$, there is a comparable factor in the scale]. Note also that, for smaller separations, the antenna would start to couple such that this would be impractical anyhow. When extending the separation of the two antennas in the original pair to $2\Delta r = 200$ m, one would have a place for approximately 2000 antennas in between. This, in turn, would then allow correlations from 10^6 pairs of antennas, where the antennas in each pair are still separated at least by $\Delta r = 100$ m. When considering that averaging of N temperature profiles obtained from N statistically independent correlation functions improves the signal-to-noise ratio of the average temperature profile by a factor $\sqrt{N}$, we can improve the signal-to-noise ratio (SNR) by a factor of 10^3. If considering the prefactors of order 1, 10 times more antennas can be used, the SNR could be improved by a factor 10^4. However, even such a large improvement is not yet sufficient to beat the low SNR on the order of $\chi^{3/2} \simeq 10^{-5}$. It is quite likely, however, that a displacement of an antenna also in the x-direction by a distance on the order of $\lambda/(2\pi)$ leads to a completely decorrelated correlation function. If so, one might gain another factor, up to 10^3 in the SNR, by considering quasi-1D antenna arrangements, with a width in the x-direction on the order of 10 m. In the latter case, one should then be able (after averaging temperature profiles obtained from some 10^{14} correlation functions from that many pairs of antennas) to achieve an SNR of 10^2 and, hence, an RR on the order of a few degrees Kelvin. However, it is obvious that the effort for doing so is huge, and the same geometrical and radiometric resolution might be achievable more easily with other means.

Other interesting ideas of improving the SNR involve using focusing antennas for increasing the flux and/or exploiting higher order correlation functions as well, but these are beyond the scope of the present investigation.

VII. DISCUSSION

We examined the fundamental feasibility of a new type of passive remote microwave imaging of a 2D scenery with a satellite having only a 1D antenna array, arranged perpendicular to the direction of flight of the satellite. We analyzed the simplest possible configuration of only two antennas. The scheme is based on correlating Fourier components of the observed electric field fluctuations at the position of the two antennas at slightly different frequencies, ω_1 and ω_2, and leads effectively to a mapping of the 2D brightness temperature as a function of position x, y to correlations as function of the center frequency $\omega_c = (\omega_1 + \omega_2)/2$ and the frequency difference $\Delta\omega = \omega_1 - \omega_2$. With two antennas separated by Δr, the center frequency ω_c and a satellite flying at height h, the resolution both in the x- and y-directions is on the order of $h\chi = hc/(\Delta r \omega_c)$. Only very small frequency differences lead to correlations of a finite, useful magnitude. For typical intended SMOS-NEXT values, they are on the order of, at most, 10 Hz, which, however, still has to be divided by the number of points in the x-direction that one wants to resolve within a snapshot. This implies that one must be able to measure GHz frequencies with an accuracy on the order of 1/10–1/100 Hz. The speed v_s of the satellite only enters in the maximum frequency difference useful for correlating the signals, which is given by $\Delta\omega \lesssim (\Delta r/h)(v_s/c)\omega_c$.

In the minimal situation of two antennas, the relative radiometric resolution $\sigma(T)/T$ is, for a single point source on the order of $\sqrt{\chi}$, whereas, for a uniform temperature field in the positive half plane $y > 0$ (up to some large cutoff of the size of the Earth), $\sigma(T_{\rm rec})/T_{\rm rec} \sim 1/\chi^{3/2}$, which, for standard parameters, is on the order of 10^5. We neglected, so far, the additional noise that comes from the antennas themselves, such that our results should be considered as lower bounds for $\sigma(T_{\rm rec})/T_{\rm rec}$. However, it should be kept in mind that a factor χ in $T_{\rm rec}$ estimated with the approximate analytical approach largely contributes to the $1/\chi^{3/2}$ behavior. If referring the fluctuations to the actual temperature, one finds $\sigma(T_{\rm rec})/T \sim 1/\sqrt{\chi}$, which already substantially improves the situation. A numerical investigation that gives an unbiased estimate of $T(x, y)$ should be able to decide what is the correct scaling. If the $1/\chi^{3/2}$ prevails, then such a large uncertainty would prevent a direct application of the method with just two antennas, and massive noise reduction is required. Some ideas are discussed in Sec. VI, where it was found that one can obtain statistically independent correlation functions by displacing one antenna by a distance on the order of $\lambda/2\pi$, where λ is the central wave-length. Hence, the signal-to-noise ratio $T_{\rm rec}/\sigma(T_{\rm rec})$ can be massively increased by a factor N when using the correlations from $\sim N(N-1)/2$ pairs of antennas from N antennas separated all by at least a distance on the order of $\lambda/2\pi$. However, the computational effort and the size of the overall structure seem forbiddingly large for achieving a radiometric resolution on the order of a few degrees Kelvin with a geometrical resolution on the order of 1 km.

An alternative application might be the precise localization of very strong point sources that, by far, dominate the more or less uniform background from the Earth's thermal emission. As long as one is not interested in a very precise measurement of the intensity of the source, one might localize it very precisely by using just two widely separated antennas. These antennas need not even be on board the same satellite. By having two satellites with a well-known distance separated by approximately 100 km for instance, the geometrical resolution achievable in the microwave regime would be on the order of a meter in both the x- and the y-direction, and with rather small computational effort, opening interesting perspectives for such applications. With the standard interferometry from just two antennas, one could resolve the source only in the direction perpendicular to the track of the satellite, whereas no resolution at all would be possible in the direction of the track. We agree that controlling the distance between two satellites separated by 100 km to within 10 cm is challenging but not completely unreasonable given the performance of modern global positioning systems. For the analytical analysis, we assumed that the distance is constant, but, in practice, the method can probably be extended to varying distances as long as these are known precisely as a function of time, similarly, as for radio-astronomy with phased antenna arrays.

It should also be kept in mind that the method can be easily transferred to other types of waves, sources, and media. For example, 2D (ultra-)sound imaging might be possible by observing the beating of the signals of just two moving microphones. Different physical systems can be easily mapped to each other by comparing the corresponding dimensionless parameters introduced in Sec. I.

ACKNOWLEDGMENTS

The authors thank the CESBIO SMOS team and the CNES project management, without whom this work would not have succeeded. We more particularly appreciate the technical support from François Cabot, Eric Anterrieu, Ali Khazaal, Guy Lesthiévant, and Linda Tomasini.

APPENDIX A: CURRENT FLUCTUATIONS AND TEMPERATURE

The connection between the intensity of the current fluctuations and the local temperature can be found, e.g., in Refs. 9 and 11–13. For being self-contained and relating to the notations used in this paper, we here give a short derivation of this connection. We also show that $\hat{E}_{z,\mathbf{r}}(\omega)$, in the frequency range considered, is a circularly symmetric Gaussian process.

1. Thermal radiation

We begin by recalling the energy density of electromagnetic black body radiation at frequency ω, $u(\omega) = \hbar\omega\rho(\omega) f(\omega,T)$, where $\rho(\omega) = \omega^2/(\pi^2 c^3)$ is the density of states (the number of modes between frequencies ω and $\omega + d\omega$ per volume) and $f(\omega,T) = 1/(e^{\hbar\omega/(k_B T)} - 1)$ is, the thermal Bose occupation factor, with k_B the Boltzmann constant and T the absolute temperature of the radiation field. An infinitesimal patch on the surface at position x, y with surface dA and temperature $T(x, y)$ in thermal equilibrium with the radiation field in its immediate vicinity, radiates off an amount of energy per unit time and at frequency ω given by $dA\,u\,c\cos\theta$ in direction θ with respect to the normal surface. The energy density for both polarization directions received at the position of the satellite at distance R from this patch also varies $\propto \cos\theta$, and energy conservation requires

$$du_s(\omega) = \frac{dAu(\omega)\cos\theta}{2\pi R^2} = \frac{dA\hbar\omega^3\cos\theta}{2\pi^3 c^3 R^2 (e^{\hbar\omega/(k_B T)} - 1)}. \quad \text{(A1)}$$

The Earth is a grey rather than a black body, and we, therefore, have to include the emissivity of the patch $B(x, y; \omega, \theta, \varphi)$ in the direction of the satellite given by polar and azimuthal angles. It can also depend on polarization, which we skip here for simplicity. Integration over the whole radiating surface gives the entire energy density at the position of the satellite at this frequency,

$$\begin{aligned} u_s(\omega) &= \int \frac{dx\,dy\,u}{2\pi R^2} \\ &= \int \frac{dx\,dy\hbar\omega^3\cos\theta(x,y,h)B(x,y;\omega,\theta,\phi)}{2\pi^3 c^3 (h^2+x^2+y^2)(e^{\hbar\omega/(k_B T(x,y))} - 1)}. \end{aligned} \quad \text{(A2)}$$

In the microwave regime and at temperature $T \simeq 300$ K, $\hbar\omega$ is approximately four orders of magnitude smaller than $k_B T$, such that to first order in $\hbar\omega/k_B T$, the Bose factor, $f(\omega,T) \simeq k_B T/(\hbar\omega)$, with corrections on the order of 10^{-4}. This simplifies u_s to

$$u_s(\omega) = \frac{k_B}{2\pi^3 c^3}\int dx\,dy\,\omega^2 \frac{T_B(x,y)\cos\theta(x,y,h)}{h^2+x^2+y^2}, \quad \text{(A3)}$$

where we defined the brightness temperature $T_B(x,y) \equiv T(x,y)B(x,y;\omega,\hat{k})$, i.e., the absolute temperature a black body would need to have for producing the same thermal radiation intensity at the frequency and in the direction $\hat{k}$ considered, specified explicitly by the two angles (θ,φ). At the same time, the total energy density (integrated over all frequencies) at position $\mathbf{r}_1$ of antenna 1 is $U_s = \int d\omega u_s(\omega) = \frac{\epsilon_0}{2}\langle \mathbf{E}^2(\mathbf{r}_1)\rangle$, where the average is over the thermal ensemble, but, due to ergodicity, we may also average over time, $\langle \dots \rangle_{\tau_a} = \frac{1}{\tau_a}\int_{-\tau_a/2}^{\tau_a/2}(\dots)dt$. In the end, one should take the limit $\tau_a \to \infty$. In fact, we may even average over both the thermal ensemble and time, i.e., $U_s = \frac{\epsilon_0}{2}\langle\langle \mathbf{E}^2(\mathbf{r}_1)\rangle\rangle_{\tau_a}$. Expressing then the electric field in terms of its Fourier transform, the time integral leads to a sinc-function,

$$U_s = \frac{\epsilon_0}{4\pi}\int\int \operatorname{sinc}\left[(\omega' - \omega)\frac{\tau_a}{2\pi}\right]\langle \tilde{\mathbf{E}}^*_{\mathbf{r}_1}(\omega)\tilde{\mathbf{E}}_{\mathbf{r}_1}(\omega')\rangle d\omega\, d\omega', \quad \text{(A4)}$$

with $\operatorname{sinc}(x) \equiv \sin(\pi x)/(\pi x)$. For large τ_a, the sinc-function can be replaced by $(2\pi/\tau_a)\delta(\omega - \omega')$, and we are then left with

$$U_s = \frac{\epsilon_0}{2\tau_a}\int \langle |\tilde{\mathbf{E}}_{\mathbf{r}_1}(\omega)|^2\rangle d\omega. \quad \text{(A5)}$$

Therefore, the energy density per unit frequency at frequency omega is given by $u_s(\omega) = \frac{\epsilon_0}{2\tau_a}\langle |\tilde{\mathbf{E}}_{\mathbf{r}_1}(\omega)|^2\rangle$. Together with Eq. (A3), we thus have

$$\langle |\tilde{\mathbf{E}}_{\mathbf{r}_1}(\omega)|^2\rangle = \frac{\tau_a k_B}{\pi^3 \epsilon_0 c^3}\int dx\,dy \frac{\omega^2 T_B(x,y)\cos\theta(x,y,h)}{h^2+x^2+y^2}. \quad \text{(A6)}$$

The connection to the current fluctuations is found by comparing this expression with what we obtain from Eq. (11) if we do not use (7) yet. There we set $i=j$, $\mathbf{r}_1 = \mathbf{r}_2 = (0,0,h)$, $\omega_1 = \omega_2$, and $v_s = 0$ because we are interested in the energy density in a given fixed point $\mathbf{r}_1$, identical to the original position of the antenna. This gives

$$\begin{aligned} \langle |\tilde{E}_{i,\mathbf{r}_1}(\omega)|^2\rangle = K_4 &\int_{-\infty}^{\infty} dt_1 \int_{-\infty}^{\infty} dt_2 \int_{-\infty}^{\infty} d\omega' \\ &\times \int dx\,dy \frac{\omega'^2 \langle |\tilde{j}_i(x,y,\omega')|^2\rangle}{h^2+x^2+y^2} \\ &\times e^{i(\omega-\omega')(t_1-t_2)}, \end{aligned} \quad \text{(A7)}$$

where $K_4 = K_1^2 l_c^3 d/(4\pi^2\tau_c)$, and we have already restricted the current density to the surface of the Earth, i.e., when assuming $\langle|\tilde{j}_i(\mathbf{r}',\omega')|^2\rangle = d\langle|\tilde{j}_i(x,y,\omega')|^2\rangle\delta(z)$. In practice, the time integrals that originate from the Fourier transforms will be taken over a finite time τ_F. Because the only time-dependence is in the exponential, the time integrals can be done exactly, which leads to

$$\int_{-\tau_F/2}^{\tau_F/2}\int_{-\tau_F/2}^{\tau_F/2} dt_1\, dt_2 e^{i(\omega-\omega')(t_1-t_2)} = \frac{2}{(\omega-\omega')^2}\left\{1-\cos\left[\tau_F(\omega-\omega')\right]\right\}. \quad \text{(A8)}$$

For a large τ_F, this function is highly peaked at $\omega=\omega'$ and behaves as $2\pi\tau_F\delta(\omega-\omega')$, where the prefactor may be verified by integrating both sides of the equation over ω from minus infinity to infinity. We are thus led to

$$\langle|\tilde{E}_{i,\mathbf{r}_1}(\omega)|^2\rangle = K_4 2\pi\tau_F \int dx\, dy \frac{\omega^2\langle|\tilde{j}_i(x,y,\omega)|^2\rangle}{h^2+x^2+y^2}. \quad \text{(A9)}$$

The thermal fluctuations of the electric field are isotropic in their intensity, such that one third of the energy is in a given polarization direction i, i.e., $\langle|\tilde{E}_{i,\mathbf{r}_1}(\omega)|^2\rangle = \frac{1}{3}\langle|\tilde{\mathbf{E}}_{\mathbf{r}_1}(\omega)|^2\rangle$. Inserting Eq. (A6) for the latter quantity, we are led to

$$\langle|\tilde{E}_{i,\mathbf{r}_1}(\omega)|^2\rangle = \frac{\tau_a k_B}{3\pi^3\epsilon_0 c^3}\int dx\, dy\, \frac{\omega^2 T_B(x,y)\cos\theta(x,y,h)}{h^2+x^2+y^2}. \quad \text{(A10)}$$

Comparison with Eq. (A9) allows one to identify

$$\langle|\tilde{j}_i(x,y,\omega)|^2\rangle = K_2 T_{\text{eff}}(x,y), \quad \text{(A11)}$$

with $K_2 = 32\tau_a\tau_c k_B/(3\tau_F l_c^3 d\mu_0 c)$ and $T_{\text{eff}}(x,y) \equiv T_B(x,y)\cos\theta(x,y,h)$. Thus, the current fluctuations are given directly by the brightness temperature [rescaled by the directional $\cos\theta(x,y,h)$], up to a constant prefactor. As mentioned in the Introduction, we write T for short for T_{eff} in the rest of the article. The constant prefactor depends on the time intervals for averaging and the Fourier transforms, but, in the end, we will always be interested in relative radiometric resolution, i.e., $\sigma[T(x,y)]/T(x,y)$, where $\sigma[T(x,y)]$ denotes the standard deviation of the reconstructed temperatures over the thermal ensemble of the radiation field, such that the constant prefactor cancels out.

2. Fluctuations of the reconstructed temperature profile

A Gaussian distribution of a complex jointly Gaussian random vector $z=(z_1,z_2,\ldots,z_n)\in\mathbb{C}^n$ is fully characterized by the expectation values, $E(z_i)\,\forall i$, the covariance matrix $K=E[z z^\dagger]$, and the pseudo-covariance matrix $M=E[z z^t]$. Both matrices together specify the correlations between the four different combinations of real and imaginary parts of the z_i. The Gaussian distribution is called circularly symmetric, if $P(z)$ is invariant under the transformation $z\mapsto z e^{i\phi}$ with an arbitrary real phase ϕ. One shows that a distribution is Gaussian symmetric if and only if $M=0$. This implies immediately that $E[z_i]=0\,\forall i$.[15]

The corresponding definitions and statements for complex Gaussian processes are easily obtained by replacing the discrete index i in z_i by a continuous one, e.g., a time argument, or, in our case, of $\hat{E}_{z,\mathbf{r}}(\omega)$, a 4-component real vector with a "continuous index" $\omega,\mathbf{r}$. To show that $\hat{E}_{z,\mathbf{r}}(\omega)$ is a circularly symmetric complex Gaussian process over $\omega,\mathbf{r}$, we need to prove that $0=M(\mathbf{r}_1,\mathbf{r}_2,\omega_1,\omega_2)\equiv\langle\hat{E}_{z,\mathbf{r}_1}(\omega_1)\hat{E}_{z,\mathbf{r}_2}(\omega_2)\rangle$, at least in the narrow frequency band in which we are interested. In view of Eq. (5), for this, it is enough to show that $M_J\equiv\langle\tilde{j}_{z,\mathbf{r}_1}(\omega_1)\tilde{j}_{z,\mathbf{r}_2}(\omega_2)\rangle=0$. Expressed as Fourier transforms of the time-dependent current densities, this correlator equals

$$\langle\tilde{j}_{z,\mathbf{r}_1}(\omega_1)\tilde{j}_{z,\mathbf{r}_2}(\omega_2)\rangle = \frac{1}{2\pi}\int_{-\infty}^{\infty} dt_1\, dt_2 e^{-i(\omega_1 t_1+\omega_2 t_2)} \times\langle j_{z,\mathbf{r}_1}(t_1) j_{z,\mathbf{r}_2}(t_2)\rangle. \quad \text{(A12)}$$

The physical origin of the current fluctuations are thermal fluctuations, and the condition of the thermal equilibrium implies that the current correlator is invariant under global time translation (i.e., a shift of the origin of the time axis of t_1 and t_2 by the same amount) and, hence, depends only on t_2-t_1, $\langle j_{z,\mathbf{r}_1}(t_1)j_{z,\mathbf{r}_2}(t_2)\rangle = f(\mathbf{r}_1,\mathbf{r}_2,\tau)$, where $\tau=t_2-t_1$, and we will also use $t=(t_2+t_1)/2$. With this, we get

$$M_J = \frac{1}{2\pi}\int_{-\infty}^{\infty} dt\, e^{-i(\omega_1+\omega_2)t}\int_{-\infty}^{\infty} d\tau\, e^{-i(\omega_2-\omega_1)\tau/2} f(\mathbf{r}_1,\mathbf{r}_2,\tau) = \sqrt{2\pi}\delta(\omega_1+\omega_2)\tilde{f}[\mathbf{r}_1,\mathbf{r}_2,(\omega_2-\omega_1)/2], \quad \text{(A13)}$$

where $\tilde{f}(\mathbf{r}_1,\mathbf{r}_2,\omega)$ is the Fourier transform of $f(\mathbf{r}_1,\mathbf{r}_2,t)$ with respect to time t. The δ-function implies that M_J vanishes unless $\omega_1=-\omega_2$. But we are interested only in frequencies in the small interval $\omega_2\in[\omega_1-\Delta\omega,\omega_1+\Delta\omega]$, centered close to ω_0 on the order of 1.4 GHz. Hence, in this frequency interval, we indeed have $M_J=0$, and the complex Gaussian process $\hat{E}_{z,\mathbf{r}}(\omega)$ over $\omega,\mathbf{r}$ can be considered as circularly symmetric. In particular, it does not contain any correlator of the type EE but only of the type EE^*.

The fact that the Gaussian random processes given by $\tilde{E}_{z,\mathbf{r}_i}(\omega)$ are circularly symmetric in the narrow frequency interval considered implies that it enjoys the property [see Eq. (8.250) in Ref. 16]

$$\langle E_i E_j E_k^* E_l^*\rangle = \langle E_i E_k^*\rangle\langle E_j E_l^*\rangle + \langle E_i E_l^*\rangle\langle E_j E_k^*\rangle, \quad \text{(A14)}$$

where we have abbreviated $E_i\equiv\tilde{E}_{z,\mathbf{r}_{(i \bmod 2)}}(\omega_i)$. The correlation function contained within the large parentheses of the second line of (41), therefore, becomes

$$C_{zz}^F(\mathbf{r}_1,\mathbf{r}_1,\kappa_{13},\tilde{k}_{c13})C_{zz}^{F*}(\mathbf{r}_2,\mathbf{r}_2,\kappa_{24},\tilde{k}_{c24}), \quad \text{(A15)}$$

with $\kappa_{ij}=\Delta r(\omega_j-\omega_i)/v_s$, $\tilde{k}_{cij}=\Delta r(\omega_i+\omega_j)/(2c)\,\forall i,j$, and where we used $\langle\hat{C}^F(\mathbf{r}_1,\mathbf{r}_2,\kappa,\tilde{k}_c)\rangle = C^F(\mathbf{r}_1,\mathbf{r}_2,\kappa,\tilde{k}_c)$.

The fact that C_{zz}^F and C_{zz}^{F*} in (A15) contain the same position arguments twice indicates that we cannot evaluate it directly through Eq. (21) because the coordinate transformation to dimensionless variables based on the rescaling with Δr becomes singular. We, therefore, have to go back a step to Eq. (20), which yields

$$C_{zz}^F(\mathbf{r}_1,\mathbf{r}_1,\kappa,\tilde{k}) = K_6 e^{-i\kappa_x x_0}\int_{-\infty}^{\infty}\int_{-\infty}^{\infty} dx'\,dy'\,\frac{\tilde{T}_{0,y'}(\kappa_x)e^{-i\kappa_x' x'}}{x'^2+y'^2+h^2}, \tag{A16}$$

$$= K_6 e^{-i\kappa_x x_0}\pi\int dy'\,\frac{\tilde{T}_{0,y'}(\kappa_x)e^{-|\kappa_x|\sqrt{y'^2+h^2}}}{\sqrt{y'^2+h^2}}. \tag{A17}$$

When compared with (21), we see that this result corresponds formally to $\omega_c = 0$ in that equation, rather than $\Delta r = 0$, and (A17) is recovered by using the exact result (B2)]. We can now re-introduce dimensionless variables via the same rescaling with Δr, where Δr is still given by $\Delta r = |\mathbf{r}_2 - \mathbf{r}_1|$, and $\mathbf{r}_i$ denotes as before the positions of the two antennae at $t = 0$, only one of which still enters as argument in $C_{zz}(\mathbf{r}_1,\mathbf{r}_1,\kappa_{13},\tilde{k}_{13})$, respectively, $C_{zz}^{F*}(\mathbf{r}_2,\mathbf{r}_2,\kappa_{24},\tilde{k}_{c24})$. This gives

$$C_{zz}^F(\mathbf{r}_1,\mathbf{r}_1,\kappa,\tilde{k}) = K_6 e^{-i\kappa\tilde{x}_0}\pi\int d\eta'\,\frac{\tilde{T}_{0,\eta'}(\kappa)e^{-|\kappa|\sqrt{\eta'^2+\tilde{h}^2}}}{\sqrt{\eta'^2+\tilde{h}^2}}, \tag{A18}$$

which proves (41) in the main text with (42) and (43).

APPENDIX B: PROPERTIES OF THE INTEGRAL KERNEL

Here, we establish the behavior and relevant parameter regimes of the kernel $K(\alpha,\beta)$. Note that, from (22), we immediately obtain the relations

$$K(\alpha,\beta) = K(-\alpha,\beta) = K(\alpha,-\beta)^*. \tag{B1}$$

We, therefore, restrict the following discussion to $\alpha,\beta \geq 0$.

Unfortunately, the integral over ξ in (22) cannot be done analytically. However, we can find approximations for different cases. First consider $\beta = 0$. By using the methods of residues, one easily finds

$$K(\alpha,0) = \pi e^{-\alpha}. \tag{B2}$$

More generally, one can obtain a useful expansion for a small β by expanding $\exp\left(-i\beta/\sqrt{\xi^2+1}\right)$ into a power series, and then integrating term by term. We find

$$K(\alpha,\beta) = \sum_{n=0}^{\infty}\frac{1}{n!}\int_{-\infty}^{\infty}(-i\beta)^n\frac{e^{-i\alpha\xi}}{(\xi^2+1)^{1+\frac{n}{2}}}\,d\xi, \tag{B3}$$

$$= \sqrt{2\pi\alpha}\sum_{n=0}^{\infty}\frac{\left(-i\beta\sqrt{\alpha/2}\right)^n}{n!\,\Gamma(1+n/2)}K_{(n+1)/2}(\alpha), \tag{B4}$$

where $K_n(x)$ is the modified Bessel function of the second kind of order n. The zeroth order result (B2)] is recovered by observing that $K_{1/2}(x) = \sqrt{\frac{\pi}{2x}}e^{-x}$. For a small β, the series converges rapidly, and one can even improve the agreement with the numerically calculated kernel by re-exponentiating the first few terms. For example, up to the second order, we have a polynomial $p_0 + p_1\beta + p_2\beta^2$, which we want to write as $p_0\exp(a_1\beta + a_2\beta^2)$. By expanding the exponential in powers of β and by comparing powers up to the order β^2, one finds $a_1 = p_1/p_0$ and $a_2 = p_2/p_0 - (p_1/p_0)^2/2$. When plotted together with the exact result, the thus-obtained approximation agrees with $K(\alpha,\beta)$ for $\alpha = 2$ visibly well up to $\beta \simeq 4$, i.e., well beyond the regime $\beta \ll 1$. For the fourth order re-exponentiated form, the agreement extends up to approximately $\beta \simeq 5$. However, the exponential decay (B2) already of the zeroth order term with α indicates that, for the values of $\alpha \simeq 10^2$ to 10^3, the contribution to the η integral for values such that β is on the order of or smaller than one, can be entirely neglected.

In the opposite regime of a large β, an approximation based on a stationary phase approximation can be found. More precisely, one needs $\beta \gg \alpha$. In this case, one can treat $e^{-i\alpha\xi}/(\xi^2+1)$ as a slowly varying factor compared with the rapidly oscillating $e^{-i\beta/\sqrt{\xi^2+1}}$. The point of the stationary phase of the latter term is found at $\xi = 0$ (where the phase has a maximum). The second derivative of the phase at $\xi = 0$ equals 1. With this, we get

$$K(\alpha,\beta) \simeq \sqrt{\frac{2\pi}{\beta}}e^{i\pi/4}e^{-i\beta}, \tag{B5}$$

valid for $\beta/\alpha \gg 1$. Interestingly, the integral kernel becomes independent of α in this regime, which is a consequence of the fact that the stationary phase point is at $\xi = 0$, which thus eliminates the factor α in the phase of the prefactor. We, furthermore, see that, in this regime, there is no exponential suppression of the kernel.

For $\alpha = 0$, the kernel can be evaluated exactly,

$$K(0,\beta) = \int_{-\infty}^{\infty}d\xi\,\frac{e^{-i\frac{\beta}{\sqrt{\xi^2+1}}}}{\xi^2+1} = \pi[J_0(\beta) - iH_0(\beta)], \tag{B6}$$

where J_0 is the zeroth Bessel function, and H_0 is the zeroth Struve function. Their asymptotic behavior gives back (B5).

In Fig. 3, we plot α, β as a function of η. We see that a regime $\alpha < \beta$ exists for $\kappa < \kappa_{\mathrm{Max}}$, which defines κ_{Max} [see the discussion after Eq. (27) for its precise value]. For $\kappa \ll \kappa_{\mathrm{Max}}$, $\alpha \ll \beta$. The regime $\alpha \sim \beta \ll 1$ is also possible, but it is restricted to a tiny η interval, such that its contribution to the integral over η is negligible. For $\alpha \sim \beta \gg 1$, the stationary phase points of $\xi + (\beta/\alpha)/\sqrt{\xi^2+1}$ become relevant. Figure 3 shows the Im- and Re-parts of the six roots of the corresponding stationary phase equation. We see that, only for $(\beta/\alpha) \gtrsim 2.5$, real stationary phase points exist. However, because $\alpha \sim \beta \gg 1$ occurs for sufficiently large κ for almost all η only for $\beta < \alpha$ (see Fig. 3), the kernel is exponentially small in this regime $\alpha \sim \beta \gg 1$. Altogether, the only relevant regime is thus $\beta \gg \alpha \gg 1$.

Although the asymptotic form of the integral kernel suggests the use of the orthogonality relations of Bessel functions, inverting (20) is, nevertheless, non-trivial due to the more complicated dependence of α and β on η. However, the above asymptotic form allows one to obtain an approximate analytical inversion of the kernel, which allows for an estimation of the resulting resolution, as we now show.

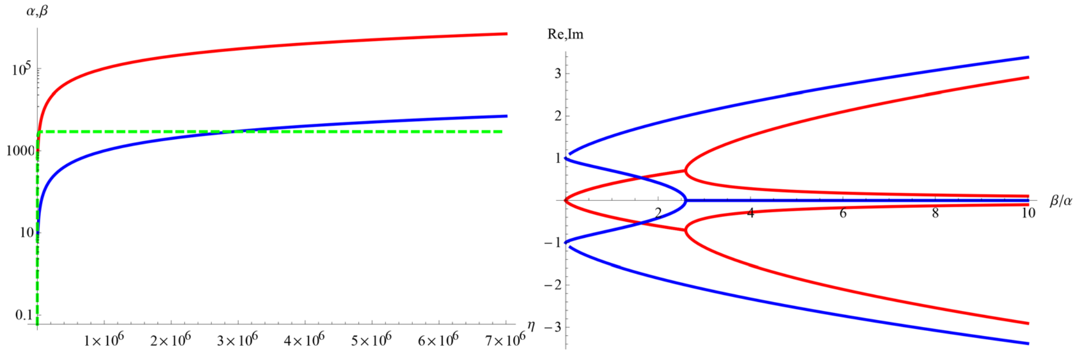

FIG. 3. (Left) α and β as functions of η. Standard parameters are used (see Sec. I), and two different values for κ_x: $\kappa_x = 10^{-5}/$ m (blue curve for α) and $\kappa_x = 10^{-3}/$ m (red curve for α); β (green dashed curve) is independent of κ_x. (Right) Real (red) and imaginary parts (blue) of the roots of the stationary phase equation in the regime $\alpha \sim \beta$ as a function of β/α.

APPENDIX C: RECONSTRUCTED IMAGE OF A POINT SOURCE

From $T(\mathbf{r}'')$ in (35) and Eq. (16), we obtain

$$\tilde{T}(\kappa,\eta) = \frac{T_0 \Delta r}{\sqrt{2\pi}}\delta(\eta-\eta_s). \tag{C1}$$

Because η is assumed to be in the allowed range for the point source considered, we can use the approximate analytical form of the integral kernel, Eq. (28), to get from Eq. (29) the correlation function

$$C_{ii}(\mathbf{r}_1,\mathbf{r}_1+\Delta r\hat{e}_y,\kappa,\tilde{k}_c) = K_6 T_0 \Delta r \frac{e^{-i\kappa\tilde{x}_0} e^{i\,\mathrm{sign}(\tilde{k}_c)\pi/4}}{\sqrt{|\tilde{k}_c|\eta_s}(\eta_s^2+\tilde{h}^2)^{1/4}} e^{-i\tilde{k}_c\frac{\eta_s}{\sqrt{\eta_s^2+\tilde{h}^2}}}\theta[\kappa_{\max}(\eta_s)-|\kappa|], \tag{C2}$$

where $\theta(x)$ is the Heaviside theta-function. When considering (34), we may define an approximative reconstructed source function suitable for sources at $\eta_s > 0$ through

$$\tilde{T}_{\mathrm{rec}}(\kappa,\eta) \equiv \mathcal{N}\mathcal{F}_{\tilde{k}_c\to\zeta}\left[C_{ii}^F(\mathbf{r}_1,\mathbf{r}_1+\Delta r\hat{e}_y,\kappa,\tilde{k}_c)\sqrt{\frac{|\tilde{k}_c|}{2\pi}}\frac{e^{i\kappa_x x_0}}{K_6}\right], \tag{C3}$$

where $\mathcal{N}$ is a normalization constant. Due to the κ-dependence of the window functions, and the ζ dependence of the integral transform compared with a simple Fourier transform of $\tilde{T}$, one cannot get a normalization constant independent of the source field. In particular, for the single point source, $\mathcal{N}$ would depend on the position of the point source. However, we use T_{rec} only for estimating the geometric and radiometric resolution. For the former, all prefactors are irrelevant. For the latter, we avoid the problem by calculating relative uncertainties of $\sigma(T_{\mathrm{rec}})/T_{\mathrm{rec}}$ only, where any prefactor cancels. Hence, we set $\mathcal{N}=1$ in the following equations.

Inverting the Fourier transform in κ leads to

$$T_{\mathrm{rec}}(x,y) = \frac{1}{2\pi K_6 \Delta r}\int_{-\infty}^{\infty} d\kappa \int_{-\infty}^{\infty} d\tilde{k}_c e^{-i\kappa(\tilde{x}-\tilde{x}_0)} e^{i\tilde{k}_c\zeta} \times C_{ii}^F(\mathbf{r}_1,\mathbf{r}_1+\Delta r\hat{e}_y,\kappa,\tilde{k}_c)\sqrt{\frac{|\tilde{k}_c|}{2\pi}}. \tag{C4}$$

This equation is valid for all sources located in the positive y plane, not necessarily point sources. When we re-express the correlation function through (29) and perform the Gaussian integral over $\tilde{k}_c$, we find a direct approximate formal relation between the FT of the original $T(x, y)$ in the upper half plane and its reconstructed image $T_{\mathrm{rec}}(x,y)$,

$$\begin{aligned} T_{\mathrm{rec}}(x,y) = {} & \frac{1}{2\pi\Delta r}\int_{-\infty}^{\infty} d\kappa \int_{-\infty}^{\infty} d\zeta' \frac{\tilde{T}\left(\kappa, \frac{\zeta'\tilde{h}}{\sqrt{1-\zeta'^2}}\right)}{\sqrt{|\zeta'|(1-\zeta'^2)}} \\ & \times e^{-i\kappa\tilde{x}} e^{-\tilde{b}^2(\zeta-\zeta')^2/4} \times \Big\{ w[\zeta_1(\kappa),\zeta_2(\kappa),\zeta'] \\ & \times \cos\left[k_{c0}(\zeta-\zeta')+\frac{\pi}{4}\right] + w[\zeta_1(\kappa),\zeta_2(\kappa),-\zeta'] \\ & \times \cos\left[k_{c0}(\zeta-\zeta')-\frac{\pi}{4}\right]\Big\}. \end{aligned} \tag{C5}$$

When using this expression, or by inserting (C2) into (32) and the resulting filtered correlation function into (C4), we find the reconstructed image of the single point source

$$\begin{aligned} T_{\mathrm{rec}}(x,y) = {} & \frac{T_0\sqrt{\zeta_s}(1-\zeta_s^2)}{\sqrt{2}\pi^{3/2}\chi\tilde{h}^2} e^{-(\zeta-\zeta_s)^2\tilde{b}^2/4} \\ & \times \cos\left[\tilde{k}_{c0}(\zeta-\zeta_s)+\frac{\pi}{4}\right]\mathrm{sinc}[\kappa_{\max}(\zeta_s)\tilde{x}/\pi], \end{aligned} \tag{C6}$$

where $\zeta_s = \eta_s/\sqrt{\eta_s^2+\tilde{h}^2}$, $\kappa_{\max}(\zeta_s) \equiv \zeta_s\sqrt{1-\zeta_s^2}/(\chi\tilde{h})$, and $\mathrm{sinc}(x) \equiv \sin(\pi x)/(\pi x)$, which proves Eq. (36) in the main text.

APPENDIX D: ADDITIONAL FREQUENCY PAIRS

Here, we show once more that using additional frequency pairs is of no use for substantially increasing the radiometric resolution. We do so by proving that, for obtaining statistically independent correlation functions, i.e., for M and V in Eqs. (61) and (60) to vanish, the second pair of frequencies ω_1', ω_2' must *not* be in S. There, however, $C_{ij}(\mathbf{r}_1,\mathbf{r}_2,\omega_1',\omega_2')$ vanishes, such that one does not obtain a second useful correlation function.

To see this, one first shows, with the help of (A14) and in a few lines of calculation, that

$$V = C_{zz}(\mathbf{r}_1, \mathbf{r}_1, \omega_1, \omega_1')C_{zz}^*(\mathbf{r}_2, \mathbf{r}_2, \omega_2, \omega_2'), \quad \text{(D1)}$$

$$M = C_{zz}(\mathbf{r}_1, \mathbf{r}_2, \omega_1, \omega_2')C_{zz}(\mathbf{r}_1, \mathbf{r}_2, \omega_1', \omega_2) . \quad \text{(D2)}$$

We have $C_{zz}(\mathbf{r}_1, \mathbf{r}_1, \omega_1, \omega_1')$ from (A18), where now $\kappa = (\omega_1' - \omega_1)\Delta r/v_s$, and, correspondingly, for $C_{zz}(\mathbf{r}_2, \mathbf{r}_2, \omega_2, \omega_2')$, where $\kappa = (\omega_2' - \omega_2)\Delta r/v_s$. Whether V and M are large or small can be judged by comparing them to the product of the standard deviations of each factor. This corresponds to calculating Pearson's product-moment coefficients[17] $V^{\text{res}} \equiv \frac{V}{\sigma(\hat{C})\sigma(\hat{C}')}$ and $M^{\text{res}} \equiv \frac{M}{\sigma(\hat{C})\sigma(\hat{C}')}$, where we define, for complex $\hat{C}$, $\sigma(\hat{C}) \equiv \sqrt{\sigma^2(\Re\hat{C}) + \sigma^2(\Im\hat{C})}$, and $\hat{C} \equiv \hat{C}_{zz}(\mathbf{r}_1, \mathbf{r}_2, \omega_1, \omega_2)$, $\hat{C}' \equiv \hat{C}_{zz}(\mathbf{r}_1, \mathbf{r}_2, \omega_1', \omega_2')$ for short. When going through the same calculation as for V, we find, after some algebra,

$$\sigma^2(\hat{C}) = C_{zz}(\mathbf{r}_1, \mathbf{r}_1, \omega_1, \omega_1)C_{zz}(\mathbf{r}_2, \mathbf{r}_2, \omega_2, \omega_2), \quad \text{(D3)}$$

$$= (\pi K_6)^2 I^2(0), \quad \text{(D4)}$$

where

$$I(\kappa) \equiv \int_{-\infty}^{\infty} \frac{\tilde{T}_{0,\eta}(\kappa)e^{-|\kappa|\sqrt{\eta^2+\tilde{h}^2}}}{\sqrt{\eta^2+\tilde{h}^2}} d\eta , \quad \text{(D5)}$$

and, hence, $I(0) = \int_{-\infty}^{\infty} \frac{\tilde{T}_{0,\eta}(0)}{\sqrt{\eta^2+\tilde{h}^2}} d\eta$. This implies

$$|V^{\text{res}}| = \left| \frac{I\left[(\omega_1' - \omega_1)\Delta r/v_s\right] I\left[(\omega_2' - \omega_2)\Delta r/v_s\right]}{I^2(0)} \right| . \quad \text{(D6)}$$

For M, we have

$$|M^{\text{res}}| = \left| \frac{C_{zz}(\mathbf{r}_1, \mathbf{r}_2, \omega_1, \omega_2')C_{zz}(\mathbf{r}_1, \mathbf{r}_2, \omega_1', \omega_2)}{C_{zz}(\mathbf{r}_1, \mathbf{r}_1, \omega_1, \omega_1)C_{zz}(\mathbf{r}_2, \mathbf{r}_2, \omega_2, \omega_2)} \right|, \quad \text{(D7)}$$

$$= \left| \frac{J(\kappa_{12'}, \omega_{c12'})J(\kappa_{1'2}, \omega_{c1'2})}{I^2(0)} \right| , \quad \text{(D8)}$$

where

$$J(\kappa_{12'}, \omega_{c12'}) \equiv \int \frac{d\eta}{\sqrt{\eta^2+\tilde{h}^2}} \times K\left(\kappa_{12'}\sqrt{\eta^2+\tilde{h}^2}, \frac{\Delta r \omega_{c12'}}{c} \frac{\eta}{\sqrt{\eta^2+\tilde{h}^2}}\right) \times \tilde{T}_{0,\eta}(\kappa_{12'}) \quad \text{(D9)}$$

with $\kappa_{12'} \equiv (\omega_2' - \omega_1)/v_s$, $\kappa_{1'2} \equiv (\omega_2 - \omega_1')/v_2$, $\omega_{c12'} \equiv (\omega_1 + \omega_2')/2$, and $\omega_{c1'2} \equiv (\omega_1' + \omega_2)/2$. From the properties of the integration kernel K, we know that $C_{zz}(\mathbf{r}_1, \mathbf{r}_2, \omega_1, \omega_2')$ vanishes if $|\omega_1 - \omega_2'| \gtrsim (\omega_1 + \omega_2')v_s/(2c\tilde{h})$ and, correspondingly, $C_{zz}(\mathbf{r}_1, \mathbf{r}_2, \omega_1', \omega_2)$. Hence, for $|M| \ll 1$ and $\omega_{1,2}$ and $\omega_{1,2}'$ all on the order of ω_0, we need $|\omega_1 - \omega_2'| \gtrsim \omega_0 v_s/(c\tilde{h})$ or $|\omega_1' - \omega_2| \gtrsim \omega_0 v_s/(c\tilde{h})$. Note that $\omega_0 v_s/(c\tilde{h}) = (1/\chi)v_s/h \gg v_s/h$.

For determining the properties of V, we consider our two previous cases of sources.

1. Case 1: Single point source

Here, we have $\tilde{T}$ independent of κ, see Eq. (C1), which, when inserted into (D5), yields

$$I(\kappa) = \frac{T_0 \Delta r}{\sqrt{2\pi}\sqrt{\eta_s^2+\tilde{h}^2}} e^{-|\kappa|\sqrt{\eta_s^2+\tilde{h}^2}} \quad \text{(D10)}$$

and, hence,

$$|V^{\text{res}}| = e^{-\frac{\Delta r}{v_s}\sqrt{\eta_s^2+\tilde{h}^2}(|\omega_1'-\omega_1|+|\omega_2'-\omega_2|)} . \quad \text{(D11)}$$

For sources at $\eta_s \sim \tilde{h}$, we, therefore, have $|V^{\text{res}}| \ll 1$ if $|\omega_1' - \omega_1| > \delta\omega$ or $|\omega_2' - \omega_2| > \delta\omega$, where $\delta\omega \equiv v_s/\left(\Delta r\sqrt{\eta_s^2+\tilde{h}^2}\right) \sim v_s/(\Delta r\tilde{h}) = v_s/h \sim 10^{-2}$ Hz.

2. Case 2: Constant temperature field in the positive upper half plane

Here, $\tilde{T}(\kappa_x, \eta)$ is given by Eq. (51). Hence, $V^{\text{res}} = 0$ as soon as $\omega_1' \neq \omega_1$ or $\omega_2' \neq \omega_2$. The $\delta(\kappa_x)$ function in (51) arises from the complete lack of structure of the temperature profile in the x-direction. More realistic is at least a cutoff at the size of the Earth, which we take as the same as in the y-direction. In this case, one finds $\tilde{T}_{\mathbf{r}'}(\kappa_x) = (\hat{y}T_0/\pi)\text{sinc}\left(\frac{\kappa_x\hat{y}}{\pi}\right)$ and, hence,

$$I(\kappa) = (\hat{y}T_0/\pi)\text{sinc}\left(\frac{\kappa_x\hat{y}}{\pi}\right)\int_0^{\hat{\eta}} \frac{d\eta}{\sqrt{\eta^2+\tilde{h}^2}} e^{-|\kappa|\sqrt{\eta^2+\tilde{h}^2}} . \quad \text{(D12)}$$

The exponential factor in the integral again indicates that V^{res} essentially vanishes if $|\omega_i' - \omega_i| \gtrsim v_s/h$ for $i = 1$ or $i = 2$.

When comparing with the situation for M, we find that, for both types of sources considered, V vanishes much more rapidly as a function of the separation of two frequencies because there is no factor $1/\chi$ multiplying v_s/h. Hence, the request for vanishing M is more restrictive.

The question of the usefulness of considering other frequency pairs can now be phrased as the following: Can one find pairs of frequencies (ω_1', ω_2'), such that $|\omega_2' - \omega_1| \gg \Delta\omega \equiv (1/\chi)v_s/h$ or $|\omega_1' - \omega_2| \gg \Delta\omega$ while still $|\omega_2' - \omega_1'| \lesssim \Delta\omega$ *for all* frequencies ω_1, ω_2 with $|\omega_2 - \omega_1| \lesssim \Delta\omega$ used in the reconstruction of a temperature profile from $C(\mathbf{r}_1, \mathbf{r}_2, \omega_1, \omega_2)$? For a single frequency pair (ω_1', ω_2'), all conditions can be easily satisfied. It is enough that both pairs (ω_1, ω_2) and (ω_1', ω_2') be inside the strip S and, at the same time, far away from each other, i.e., $|\omega_1 - \omega_1'| \gg \Delta\omega$, which implies $|\omega_2' - \omega_1| \gg \Delta\omega$ and $|\omega_1' - \omega_2| \gg \Delta\omega$ at the same time. However, the difficulty arises from the fact that we already use all pairs (ω_1, ω_2) in the full available band-width for the reconstruction of a single temperature profile. This can be seen, e.g., from Eq. (34), where we integrate over all $\tilde{k}_c = \Delta r(\omega_1 + \omega_2)/(2c)$ for recovering $\tilde{T}$. Hence, there really are no new frequency pairs that can be used for improving the signal-to-noise ratio of the reconstructed temperature profile.

The same conclusion can be arrived at more formally by calculating the correlations between temperature profiles obtained from different center frequencies. Let $T_{\text{rec}}(x, y; \omega_0)$ be the reconstructed temperature profile given by Eq. (C4), where we now keep explicit the dependence on the center frequency ω_0, hidden in that equation in the filter functions $A(\omega_1, \omega_0)$, see Eqs. (32) and (33), and $C_{ii}^F \to \hat{C}_{ii}^F$ is understood, so as to get the temperature profile from a single realization of the noise process. We define the correlation function

$$K[T_{\rm rec}(\omega_{01}), T_{\rm rec}(\omega_{02})] \equiv \langle T_{\rm rec}(x, y; \omega_{01}) T_{\rm rec}(x, y; \omega_{02})\rangle - \langle T_{\rm rec}(x, y; \omega_{01})\rangle\langle T_{\rm rec}(x, y; \omega_{02})\rangle, \tag{D13}$$

and its renormalized dimensionless version

$$K_{\rm rel}[T_{\rm rec}(\omega_{01}), T_{\rm rec}(\omega_{02})] \equiv K[T_{\rm rec}(\omega_{01}), T_{\rm rec}(\omega_{02})] / K[T_{\rm rec}(\omega_{01}), T_{\rm rec}(\omega_{01})] \tag{D14}$$

that satisfies $K_{\rm rel}[T_{\rm rec}(\omega_{01}), T_{\rm rec}(\omega_{01})] = 1$. We have

$$\begin{aligned} K[T_{\rm rec}(\omega_{01}), T_{\rm rec}(\omega_{02})] &= \left(\frac{1}{2\pi K_6 \Delta r}\right)^2 \int d\kappa_1\, d\kappa_2\, d\tilde{k}_{c1}\, d\tilde{k}_{c2} \frac{\sqrt{|\tilde{k}_{c1}\tilde{k}_{c2}|}}{2\pi} \\ &\times e^{-i(\kappa_1-\kappa_2)(\tilde{x}-\tilde{x}_0)} e^{i(\tilde{k}_{c1}-\tilde{k}_{c2})\zeta} F\left(\tilde{k}_{c1}, \tilde{k}_{c0}^{(1)}, \frac{\tilde{b}}{\sqrt{2}}\right) \\ &\times F\left(\tilde{k}_{c1}, \tilde{k}_{c0}^{(2)}, \frac{\tilde{b}}{\sqrt{2}}\right) \\ &\times [\langle \hat{C}_{zz}(\mathbf{r}_1, \mathbf{r}_2, \omega_1, \omega_2) \hat{C}_{zz}^*(\mathbf{r}_1, \mathbf{r}_2, \omega_1', \omega_2')\rangle \\ &- \langle \hat{C}_{zz}^*(\mathbf{r}_1, \mathbf{r}_2, \omega_1, \omega_2)\rangle \langle \hat{C}_{zz}(\mathbf{r}_1, \mathbf{r}_2, \omega_1', \omega_2')\rangle], \end{aligned} \tag{D15}$$

where $\kappa_1 = (\omega_2 - \omega_1)\Delta r/v_s$, $\kappa_2 = (\omega_2' - \omega_1')\Delta r/v_s$, $\tilde{k}_{c1} = (\omega_1 + \omega_2)\Delta r/(2c)$, $\tilde{k}_{c2} = (\omega_1' + \omega_2')\Delta r/(2c)$, $\tilde{k}_{c0}^{(i)} = \omega_0^{(i)}$ $(i = 1,\ 2)$, $F\left(\tilde{k}_c, \tilde{k}_{c0}, \frac{\tilde{b}}{\sqrt{2}}\right) = A(\omega_1, \omega_0) A^*(\omega_2, \omega_0)$ with $\tilde{k}_{c0} = \Delta r \omega_0 / c$ [see Eq. (31)], and we used $T_{\rm rec} \in \mathbb{R}$. We evaluate $K[T_{\rm rec}(\omega_{01}), T_{\rm rec}(\omega_{02})]$ for the case of constant temperature in the upper half plane. By using (60) and (52), and by switching momentarily to integration variables $\omega_1, \omega_2, \omega_1', \omega_2'$ and then back to $\kappa_1 \tilde{k}_{c1}$, we are led to

$$K[T_{\rm rec}(\omega_{01}), T_{\rm rec}(\omega_{02})] = \frac{T_0^2 v_s}{2\pi c} \int d\kappa_1\, d\tilde{k}_{c1} |\tilde{k}_{c1}| e^{2i\zeta\tilde{k}_{c1}} \times F\left(\tilde{k}_{c1}, \tilde{k}_{c0}^{(1)}, \frac{\tilde{b}}{\sqrt{2}}\right) F\left(\tilde{k}_{c1}, \tilde{k}_{c0}^{(2)}, \frac{\tilde{b}}{\sqrt{2}}\right). \tag{D16}$$

The integral is clearly real, as it should be. The integral over κ_1 leads, when integrated, from $-\infty$ to ∞, to a divergent factor, but that factor cancels [together with the remaining prefactor $T_0^2 v_s/(2\pi c)$] when we consider the re-scaled version of the correlation function $K_{\rm rel}[T_{\rm rec}(\omega_{01}), T_{\rm rec}(\omega_{02})]$. If we set $\tilde{k}_{c0}^{(2)} = \tilde{k}_{c0}^{(1)} + \delta\tilde{k}_{c0}$, it is clear that the only remaining scale for $\delta\tilde{k}_{c0}$ is $\tilde{b}/\sqrt{2}$. The remaining integral over $\tilde{k}_{c1}$ in (D16) can, in fact, be evaluated analytically. The result is too cumbersome to be reported here, but plotting it as a function of $\delta\tilde{k}_{c0}$ shows that, indeed, the correlations decay only on a scale on the order of $\tilde{b}$. This proves that, by shifting the center frequency within the available bandwidth, one cannot gain independent estimates of $T_{\rm rec}$ that would allow one to improve substantially the signal-to-noise ratio.

[1]A. R. Thompson, J. M. Moran, J. George, and W. Swenson, *Interferometry and Synthesis in Radio Astronomy*, 2nd ed. (Wiley-VCH, 2001).
[2]Y. H. Kerr, P. Waldteufel, J.-P. Wigneron, J.-M. Martinuzzi, J. Font, and M. Berger, IEEE Trans. Geosci. Remote Sens. **39**, 8 (2001).
[3]Y. Kerr, A. Al-Yaari, N. Rodriguez-Fernandez, M. Parrens, B. Molero, D. Leroux, S. Bircher, A. Mahmoodi, A. Mialon, P. Richaume, S. Delwart, A. Al Bitar, T. Pellarin, R. Bindlish, T. Jackson, C. Rüdiger, P. Waldteufel, S. Mecklenburg, and J. Wigneron, Remote Sens. Environ. **180**, 40–63 (2016).
[4]Y. H. Kerr, P. Waldteufel, J.-P. Wigneron, S. Delwart, F. Cabot, J. Boutin, M.-J. Escorihuela, J. Font, N. Reul, C. Gruhier, S. E. Juglea, M. R. Drinkwater, A. Hahne, M. Martin-Neira, and S. Mecklenburg, Proc. IEEE **98**(5), 666–687 (2010).
[5]A. Camps and C. Swift, IEEE Trans. Geosci. Remote Sens. **39**, 1566–1572 (2001).
[6]D. Braun, Y. Monjid, B. Rougé, and Y. Kerr, Meas. Sci. Technol. **27**, 015002 (2016).
[7]J. Jackson, *Classical Electrodynamics*, 3rd ed. (Wiley, 1999).
[8]Y. H. Kerr, P. Waldteufel, P. Richaume, J. P. Wigneron, P. Ferrazzoli, A. Mahmoodi, A. A. Bitar, F. Cabot, C. Gruhier, S. E. Juglea, D. Leroux, A. Mialon, and S. Delwart, IEEE Trans. Geosci. Remote Sens. **50**(5), 1384–1403 (2012).
[9]E. A. Sharkov, *Passive Microwave Remote Sensing of the Earth: Physical Foundations* (Springer, Berlin/New York/Chichester, UK, 2003).
[10]L. D. Landau, E. M. Lifshitz, and L. P. Pitaevskii, *Statistical Physics*, 13 ed. (Pergamon Press, Oxford, 1980).
[11]S. M. Rytov and E. Herman, *Theory of Electric Fluctuations and Thermal Radiation* (Electronics Research Directorate, Air Force Cambridge Research Center, Air Research and Development Command, U.S. Air Force, Bedford, MA, 1959).
[12]S. M. Rytov, Y. A. Kravtsov, and V. I. Tatarskii, *Principles of Statistical Radiophysics* (Springer-Verlag, Berlin, 1989).
[13]R. Carminati and J.-J. Greffet, Phys. Rev. Lett. **82**, 1660–1663 (1999).
[14]Y. Monjid, B. Rougé, Y. Kerr, and D. Braun "Numerical investigations of Fourier-Correlation Imaging" (unpublished).
[15]R. G. Gallager "Circularly-Symmetric Gaussian random vectors" (unpublished).
[16]H. H. Barrett and K. J. Myers, *Foundations of Image Science* (Wiley, 2003).
[17]K. Pearson, Proc. R. Soc. London **58**, 240–242 (1895).